Modern radio engineering and telecommunication systems

Современные радиотехнические и телекоммуникационные системы

UDC 621.37 + 004.52
https://doi.org/10.32362/2500-316X-2024-12-1-30-58

RESEARCH ARTICLE

Software-architectural configuration of the multifunctional audio digital signal processor module for signal mediatesting of audio devices

Andrey V. Gevorsky [@], Mikhail S. Kostin, Konstantin A. Boikov

MIREA – Russian Technological University, Moscow, 119454 Russia
[@] Corresponding author, e-mail: x33590@gmail.com

Abstract

Objectives. The aim of this study is to develop and analyze parameters for a multifunctional audio module based on the ADAU1701 audio digital signal processor in the *SigmaStudio* environment. This will be used for testing audio devices in the following modes: routing of balanced and unbalanced audio channels according to the differential scheme Di-Box/R Di-Box; spatiotemporal and dynamic audio processing; three-band monochannel cross-separation with independent equalization; and correction of the frequency response of the audio channel with tracking notch auto-suppression of electro-acoustic positive feedback in a given spectral band.

Methods. Visual-graphical architectural programming of audio modules in the *SigmaStudio* and *Flowstone*, as well as algorithms for real-time signal audio measurements and analysis of experimental data in the *REW* and *Soundcard Oscilloscope* are used.

Results. The characteristics of the Di-Box/R Di-Box circuit were studied, in order to estimate the effect of differential signal conversion on the signal-to-noise ratio in the audio signal path. The characteristics of the reverberation and saturation submodules were established. Furthermore, the effect of equalization modes on the frequency response correction of a studio audio monitor was determined. The paper also studied the effect of an audio compressor on the dynamic range and the level of the output signal. The experimental results of the submodule for compensating the frequency response of an audio monitor using matched filtering were established, and the spectral characteristics of the submodule for automatic suppression of electro-acoustic positive feedback were obtained.

Conclusions. The software architecture of a multifunctional audio module based on the ADAU1701 audio digital signal processor for testing and debugging media devices in a given spectral-dynamic and spectral-temporal ranges was designed. Balanced routing allows the effect of noise induced into the audio channel to be reduced 20-fold, thus enabling calibration of pickup audio devices. The audio signal processing submodule provides: compression response in the dynamic range from −27 to 18.6 dB with the possibility of equalization parameterization in the range of 0.04–18 kHz; reverberation response in the range from 0.5–3000 ms; audio-channel cross-division into 3 with the ability to adjust the amplitude-frequency response in the dynamic range from −30 to 30 dB. The auto-correction submodule of the amplitude-frequency response allows the dynamic nonuniformity of the amplitude-frequency response to be reduced by 40 dB. The auto-suppression submodule of electro-acoustic positive feedback provides notch formant suppression up to −100 dB with an input dynamic range from −50 to 80 dB.

Keywords: audio module, ADSP, ADAU1701, visual-graphic programming, software-defined architecture, audio-visual signal processing, audio signal, media-testing

• **Submitted:** 13.03.2023 • **Revised:** 20.04.2023 • **Accepted:** 18.12.2023

For citation: Gevorsky A.V., Kostin M.S., Boikov K.A. Software-architectural configuration of the multifunctional audio digital signal processor module for signal mediatesting of audio devices. *Russ. Technol. J*. 2024;12(1):30–58. https://doi.org/10.32362/2500-316X-2024-12-1-30-58

Financial disclosure: The authors have no a financial or property interest in any material or method mentioned.

The authors declare no conflicts of interest.

НАУЧНАЯ СТАТЬЯ

Программно-архитектурная конфигурация многофункционального ADSP-модуля сигнального медиатестирования аудиоустройств

А.В. Геворский [@], **М.С. Костин**, **К.А. Бойков**

МИРЭА – Российский технологический университет, Москва, 119454 Россия
[@] *Автор для переписки, e-mail: x33590@gmail.com*

Резюме

Цели. Цель статьи – программно-архитектурная разработка и параметрический анализ многофункционального аудиомодуля на базе ADSP-процессора (audio digital signal processor) ADAU1701 в среде *SigmaStudio* для тестирования аудиоустройств в следующих режимах: маршрутизация балансных и небалансных аудиоканалов по дифференциальной схеме «Di-Box/R Di-Box»; пространственно-временная и динамическая аудиообработка; трехполосное моноканальное кросс-разделение с независимой эквализацией; коррекция амплитудно-частотной характеристики (АЧХ) аудиоканала со следящим режекторным автоподавлением электроакустической положительной обратной связи (ПОС) в заданной спектральной полосе.

Методы. Использованы методы визуально-графического архитектурного программирования аудиомодулей в программных средствах *SigmaStudio* и *Flowstone*, алгоритмы сигнальных аудиоизмерений и анализа экспериментальных данных в *REW* и *Soundcard Oscilloscope*.

Результаты. Исследованы характеристики схемы «Di-Box/R Di-Box» для оценки влияния дифференциального преобразования сигнала на отношение сигнал/шум в аудиоканале. Приведены характеристики субмодулей реверберации и сатурации. Показано влияние режимов эквализации на коррекцию АЧХ студийного аудиомонитора. Исследовано воздействие аудиокомпрессора на динамический диапазон и уровень выходного сигнала. Проведены результаты экспериментального исследования субмодуля компенсационной коррекции АЧХ аудиомонитора при помощи согласованной фильтрации, а также получены спектральные характеристики субмодуля автоподавления электроакустической ПОС.

Выводы. Разработана программная архитектура многофункционального аудиомодуля на ADSP-процессоре ADAU1701 для тестирования и отладки медиаустройств в заданном спектрально-динамическом диапазоне. Балансная маршрутизация в 20 раз снижает влияние наводимых на аудиоканал шумов, что позволяет калибровать звукоснимающие аудиоустройства. Субмодуль аудиообработки обеспечивает компрессионную характеристику с динамическим диапазоном от −27 до 18.6 дБ с возможностью эквализационной параметризации в диапазоне 0.04–18 кГц; реверберационную характеристику в диапазоне 0.5–3000 мс; аудиоканальное кросс-разделение на 3 частотных поддиапазона с регулировкой АЧХ в динамическом диапазоне от −30 до 30 дБ. Субмодуль автокоррекции АЧХ позволяет снизить на 40 дБ динамическую неравномерность АЧХ. Субмодуль автоподавления электроакустической ПОС обеспечивает режекторное формантоподавление до −100 дБ при входном динамическом диапазоне от −50 до 80 дБ.

Ключевые слова: аудиомодуль, ADSP, ADAU1701, визуально-графическое программирование, программно-конфигурируемая архитектура, аудиовизуальная обработка сигналов, аудиосигнал, медиатестирование

• **Поступила:** 13.03.2023 • **Доработана:** 20.04.2023 • **Принята к опубликованию:** 18.12.2023

Для цитирования: Геворский А.В., Костин М.С., Бойков К.А. Программно-архитектурная конфигурация многофункционального ADSP-модуля сигнального медиатестирования аудиоустройств. *Russ. Technol. J.* 2024;12(1):30–58. https://doi.org/10.32362/2500-316X-2024-12-1-30-58

Прозрачность финансовой деятельности: Авторы не имеют финансовой заинтересованности в представленных материалах или методах.

Авторы заявляют об отсутствии конфликта интересов.

INTRODUCTION

The development and operation of radio-electronic devices and device-applications for digital processing of audio signals based on the specialized architecture of ADAU audio processors (Analog Devices, Inc., USA)[1] using virtual studio technology (VST) are very relevant. They are widely used in producing mixing consoles, audio effects processors, and means of dynamic, frequency, spatial-temporal, and signal audio correction. The study covers the area of signal radio acoustics along with audio-visual systems and technologies including in-circuit media testing and studies the characteristics of audio paths of audio digital signal processors (ADSP) (Fig. 1) [1].

In this paper, we set out to create a digital architecture for the multifunctional laboratory audio module in the *SigmaStudio*[2] environment, and analyze its characteristics in the aims of resolving the specialized tasks of debugging and studying the multimedia devices and complexes [2]. These tasks include: switching and transformation of balanced and unbalanced audio paths; studying the parametric impact of dynamic and spatial-temporal processing effects on audio signal; creation of submodule architecture for automatic correction of the amplitude-frequency response (AFR) of audio monitors in diffuse sound field; creation of submodule architecture for the automatic (tracking) suppression of electroacoustic positive feedback; and creation of submodule architecture of the three-band crossover with independent graphic

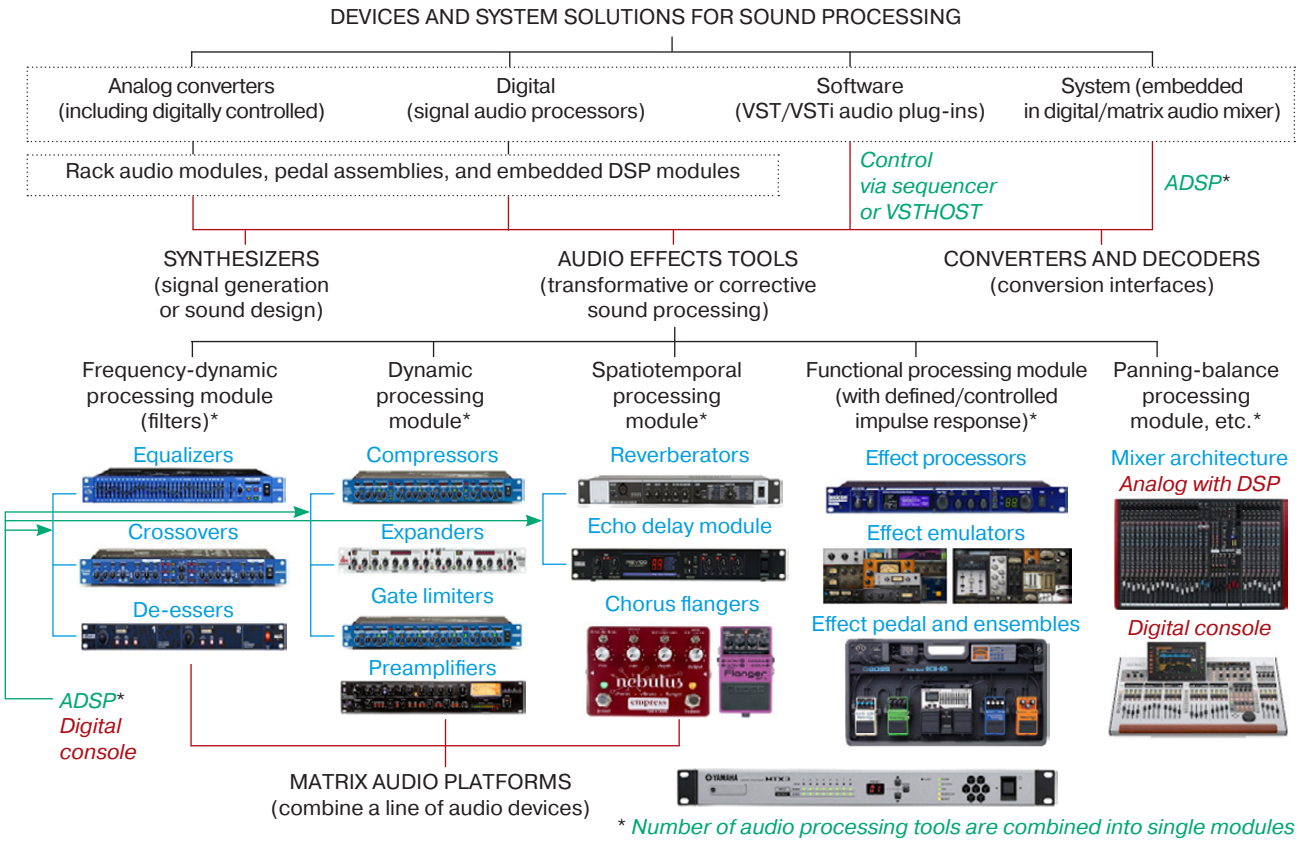

Fig. 1. ADSP classification

[1] https://www.analog.com/ADAU1701. Accessed November 10, 2022.
[2] https://wiki.analog.com/resources/tools-software/sigmastudio. Accessed February 20, 2023.

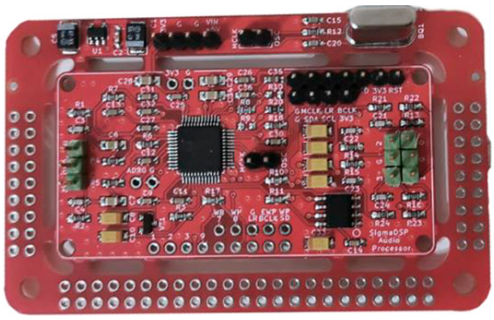

Fig. 2. ADAU1701 ADSP processor

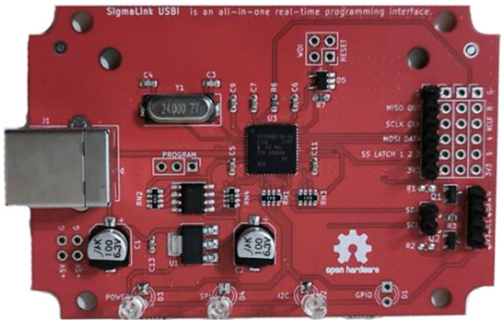

Fig. 3. SigmaLink-USBi programmer

equalization in low/mid/high-frequency (LF/MF/HF) audio ranges with specified parameterization of frequency spectrum and corresponding goodness and gain/attenuation coefficients.

The software architecture for the audio module is based on the *SigmaStudio* environment and uses the ADAU1701 audio processor (Fig. 2) encoded by the SigmaLink-USBi programmer (Analog Devices, Inc.) via I2C interface (Fig. 3). The audio module has a non-volatile EEPROM M24C64 memory manufactured by STMicroelectronics (France), 2 analog inputs with analog-to-digital converter (ADC) and 4 outputs with digital-to-analog converter (DAC) connected to JACK-Audio connectors of the stereo/mono configuration, respectively. The module is powered by a programmer with an output voltage of 3.3 V. The dynamic ranges and signal-to-noise ratio (SNR) of the 32-bit ADC/DAC are 100/104 dB, respectively. The signal audio processor is clocked by the external 12.288 MHz quartz resonator and is controlled (broadcasted) in real-time from the *SigmaStudio* visual-graphic design environment. The ADAU1701 is capable of operating with sampling frequency up to 192 kHz (with the specified clocking mode in the multifunctional audio module design being 48 kHz) [2].

The circuitry for the ADAU1701 processor of the signal audio module is shown in Fig. 4 [2]. On processor ports 2/4 (ADC inputs), there are resistor capacitor (RC) bandpass filters cutting constant and HF components out of the signal [3]. The circuit audio signal outputs correspond to ports 43–46 connected through RC bandpass filters.

The following pins and buses are brought out to the audio interface connector of the I2S serial bus (ensuring communication between the audio module and the programmer): G is GND, MCLK is 32 pin of the ADAU1701 chip, LR is MP4, BCLK is MP5, SDATA is MP0, 3V3 is 3.3 V power supply, and RST is RESET (Fig. 4).

The software and architectural configuration of the multifunctional ADSP-audio module consisting of 5 system switchable submodules is shown in Fig. 5. The signal audio module has 2 physical JACK-Audio inputs Input1 (Fig. 5, item *1*) connected via ADC to the first submodule. This is the R Di-Box reverse direct box (Fig. 5, item *2*) which performs switching of balanced (differential) and unbalanced lines. The protection of the audio system against input level overload is provided by the Limiter1 digital block (Fig. 5, item *3*) with a specified limitation from −24 up to +24 dB. The input level of the audio signal is controlled by the Single1 fader power controller within the range from −30 up to +30 dB. The selected audio module path is rooted on the '1 × N – 1' digital switch (Fig. 5, item *5*), as follows: the top position is adding the Effects audio submodule to the audio path (Fig. 5, item *6*); the second from top position is the audio signal pass-through mode (Fig. 5, item *7*); the third from top position is adding the AutoCorrection submodule to the audio path (Fig. 5, item *8*); and the fourth position is adding the Crossover submodule to the audio path (Fig. 5, item *9*). The first three cross-routes lead to S Mixer1 signal mixer (Fig. 5, item *10*) allowing controlling the dynamic level of the output signal within the range from −30 up to +6 dB. In this case, the audio signal from the Crossover submodule output is fed directly to DAC2 and DAC3 physical outputs and through the Add2 addition block to the DAC1 output (Fig. 5, item *14*).

The S Mixer1 signal mixer is connected to the switch '1 × N – 2' (Fig. 5, item *11*) which allows the routing of the output audio signal to be selected between balanced and unbalanced lines. In the upper position, the signal is switched to the Di-Box paraphase submodule (direct box) (Fig. 5, item *12*) from where the direct signal goes to the DAC0 physical output. The inverted signal (with a phase shift of 180°) goes to the DAC1 output. In the second case, the signal goes to the DAC0 physical output. Add1 and Add2 auxiliary addition blocks (Fig. 5, item *13*) allow the number of required pins of the audio module functional architecture circuit to be reduced.

The submodules (Fig. 5, items *2*, *6*, *8*, *9*, and *12*), the numerical analytics of which are outlined in [4], define the Box architecture of the multifunctional audio module and form an independent software-defined configuration.

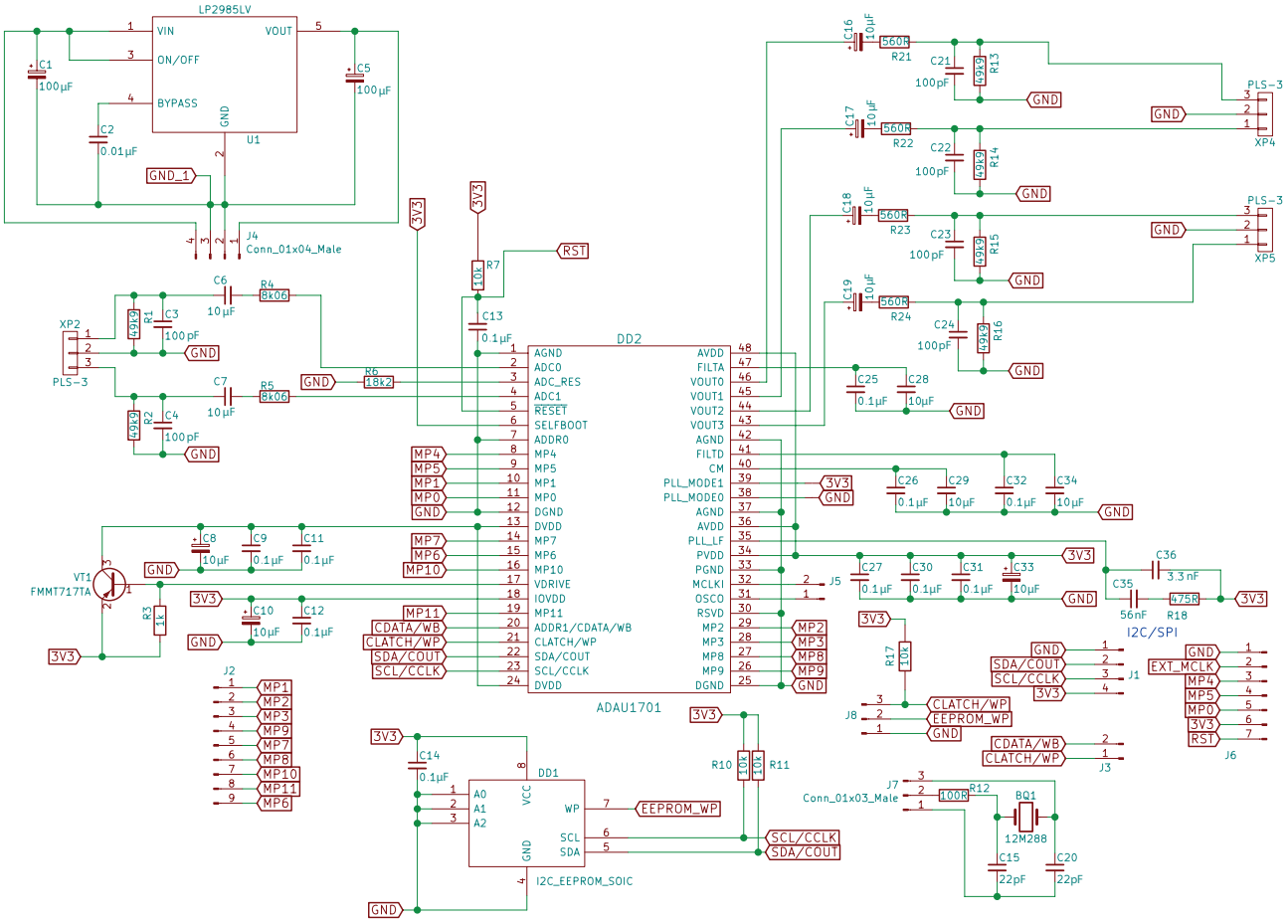

Fig. 4. Circuit architecture of the ADAU1701 audio processor[3]. The circuit element designations used here and in the following figures correspond to the designations adopted in GOST 2.710-81[4]

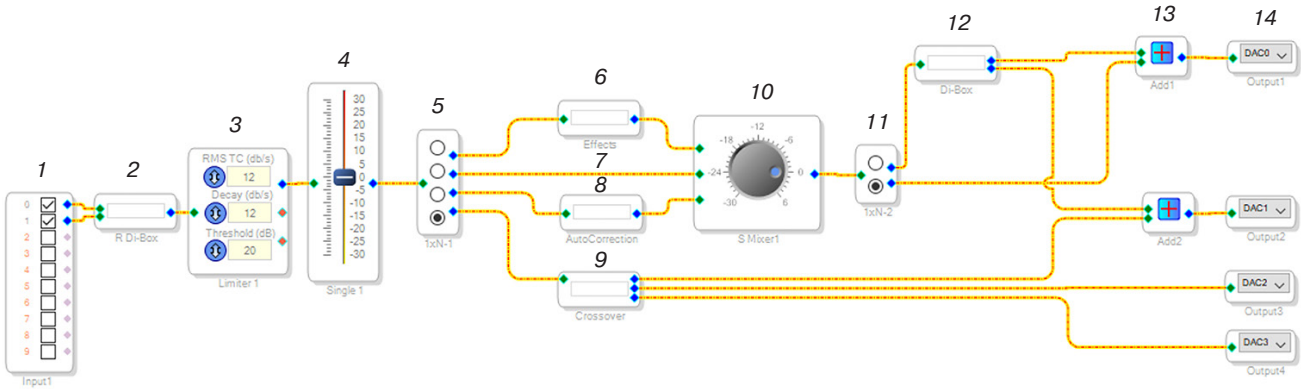

Fig. 5. Software-architectural configuration of ADSP module: *1* is Input1; *2* is R Di-Box submodule; *3* is Limiter1; *4* is Single1 input power controller; *5* is digital switch '1 × N – 1'; *6* is Effects audio submodule; *7* is audio through-pass mode; *8* is AutoCorrection submodule; *9* is Crossover submodule; *10* is S Mixer1 signal mixer; *11* is digital switch '1 × N – 2'; *12* is Di-Box submodule; *13* is Add1 and Add2 addition blocks; *14* is 'DAC0, 1, 2, 3' outputs

[3] Analog Devices. ADAU1701 Datasheet. 43 p. https://pdf1.alldatasheet.com/datasheet-pdf/view/159293/AD/ADAU1701.html. Accessed February 20, 2023.

[4] GOST 2.710-81. *Interstate Standard. Unified system for design documentation. Alpha-numerical designations in electrical diagrams*. Moscow: Izd. Standartov; 1985 (in Russ.).

1. STUDYING AND ANALYZING THE CHARACTERISTICS OF DI-BOX/R DI-BOX SUBMODULES

When an audio signal is transmitted over an unbalanced coaxial cable, the interference noise induced in the channel including interference from other audio lines of multicore switching can result in a significant decrease in SNR [4]. In this case, it would be sensible to use differential phase-symmetric lines with mono-balanced switching, for example, between an audio console and an audio device included in the line This would form a Di-Box circuit, as shown in Fig. 6, where switching is performed by means of TRS-TRS (tip, ring, sleeve) or TRS-XLR (external line return) connections.

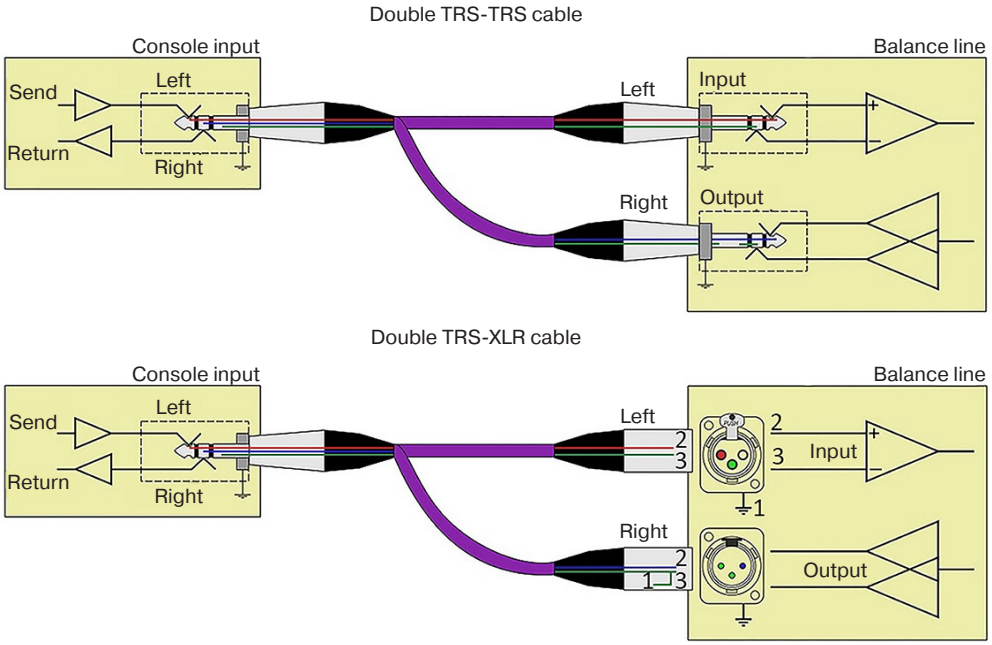

(a)

(b)

Fig. 6. Mono-balanced implementation of TRS-connector audio routing: (a) in-circuit return/send audio line (with built-in balanced audio device circuit at the input/output); (b) embedding an intermediate analog Di-Box transformer in the line with the ability to select (switch) the ground of the source (audio mixer) or receiver (audio monitor, etc.) [6]

Thus, the software-defined circuit of R Di-Box submodule is implemented at the input of the multifunctional audio module (Fig. 7a). This allows for the connection of a balanced line, for example, from an audio mixing console to a stage box [5]. One of the input channels passes through the submodule unchanged, while the second is phase inverted. Then at the receiver, the second channel signal is subtracted from the first channel signal, in order to compensate for in-phase interference swept into the differential line. In the case of an unbalanced connection, no audio signal is fed to the second channel.

The Di-Box submodule is installed at the ADSP module output (Fig. 7b). This allows the unbalanced mono signal to be converted into balanced–differential one necessary for compensation of additive noise induced on the audio path line. Using this submodule in the test mode is of practical interest when analyzing the effectiveness of noise immunity of audio systems upon the impact of external electromagnetic interference and noise exceeding −20 dB on the coaxial TRS audio line[5].

In order to study the time-response characteristics of the Di-Box submodule, a test sinusoidal signal with an amplitude of 35 mV at tone frequency of 1 kHz generated by a virtual signal generator equipped with the *Soundcard Oscilloscope* software [7] is fed to the input. Additive noise is added to this broadband with normal distribution. The experimental circuit (Fig. 8) uses the Xenyx X1622USB analog mixing console (Behringer, Germany) with mono channel panning capability as a SNR mixer. This is necessary because the two audio signals received from the stereo TRS output of the submodule (used in the balanced routing mode) require strictly separation with respect to panning. Interference located in the center of the stereo panning should be added for equal dynamic effect on both balanced channels.

The received differential signal goes through the coaxial line to R Di-Box submodule (second audio module implementing the circuit for balanced signal reception) based on the auxiliary ADSP audio module. Here it is converted into a single-channel signal and sent to the audio interface sound card. An oscillogram of the signal with compensated interference is recorded there (Fig. 9) using the *Soundcard Oscilloscope* software [5].

Analysis of the oscillograms depicted in Figs. 9c, 9d, and 9f shows that the balanced connection increases SNR by 26 dB. However, this scheme does not allow for compensation of the independent interferences induced on each channel separately.

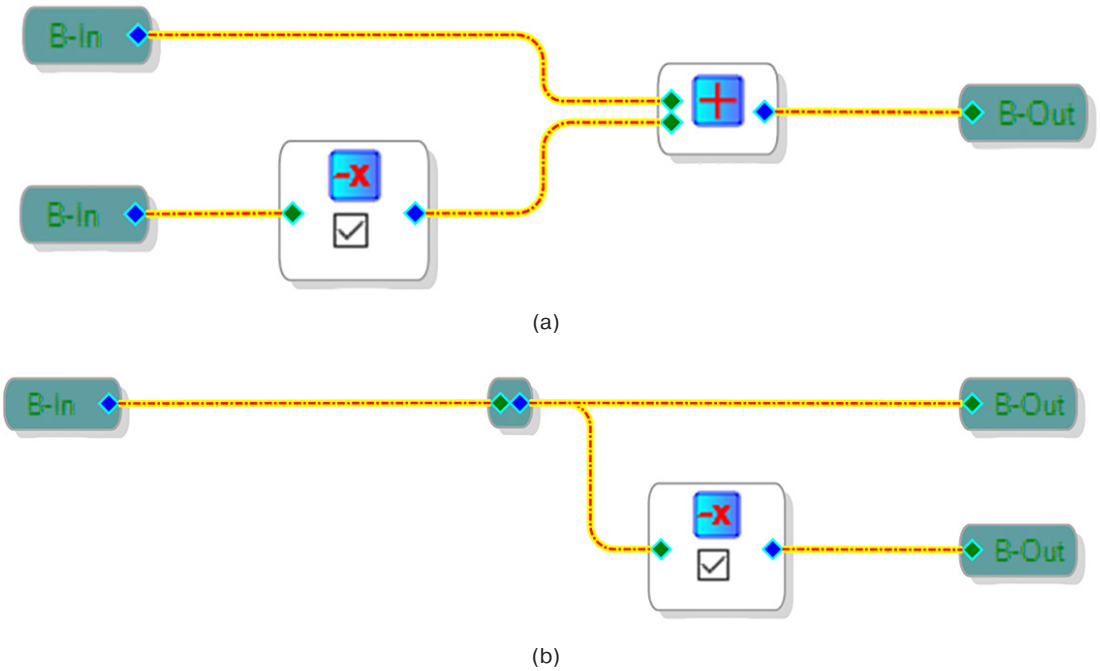

Fig. 7. Software-defined circuit of Di-Box/R Di-Box submodule combination based on ADAU1701: (a) R Di-Box module functional implementation; (b) Di-Box module functional implementation

[5] Applied Research and Technology (ART). dPDB Owner's Manual. 2 p. https://artproaudio.com/framework/uploads/2018/06/om_dpdb.pdf. Accessed February 20, 2023.

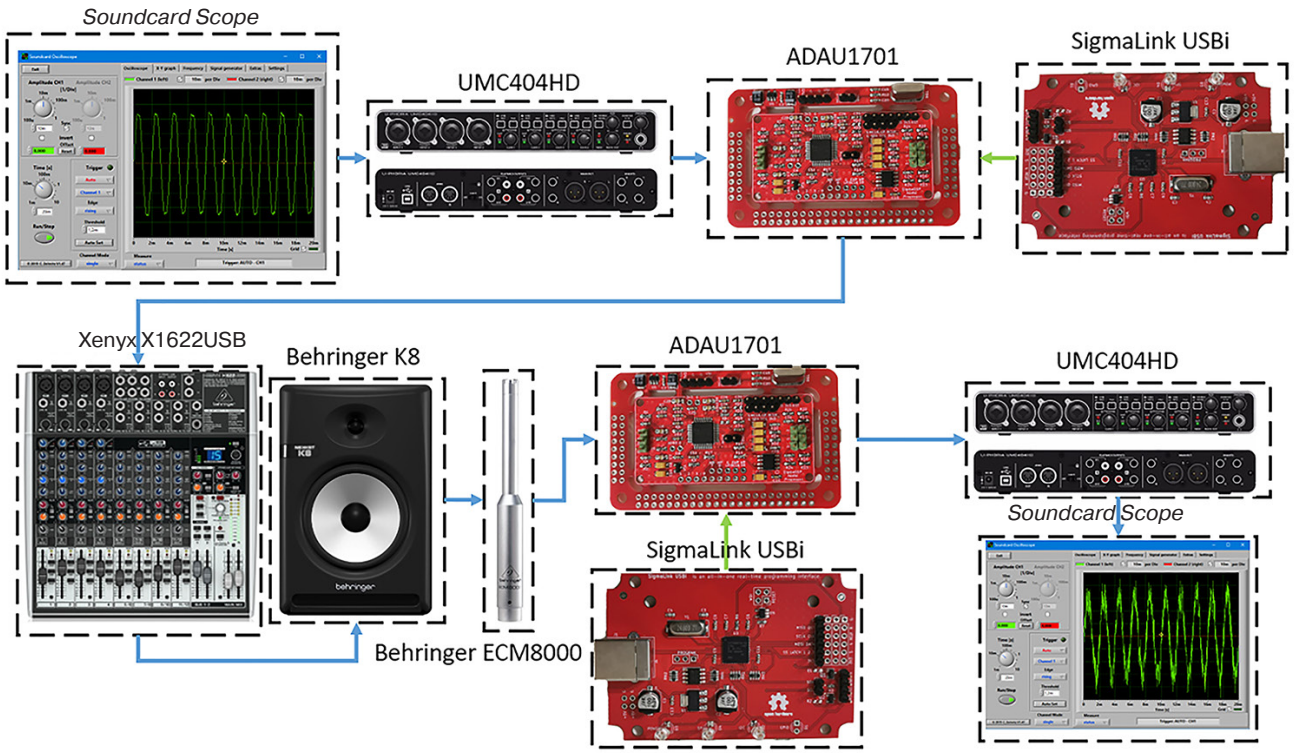

Fig. 8. Scheme of the experimental research on the balanced line submodule for suppressing broadband additive interference in TRS audio line. Behringer UMC404HD is audio interface; Behringer K8 is studio audio monitor; and Behringer ECM8000 is measuring microphone

2. DEVELOPING, ANALYZING, AND PARAMETERIZING THE CHARACTERISTICS OF SUBMODULE OF THE THREE-BAND CROSSOVER WITH INDEPENDENT GRAPHIC EQUALIZATION

The signal crossover is a multiband filter which divides audio signal into two or more frequency sub-bands adapted to the effective operation of electrodynamic cones designed for operation in different frequency bands [8]. The architecture of the circuit for the Crossover digital submodule implemented in the project allows the audio signal to be divided into three bandwidth channels of audio frequencies: low (40–250 Hz); middle (0.25–3 kHz); and high (3–18 kHz).

The three-band crossover submodule consists of a Crossover1 pre-equalization block (Fig. 10a, item *1*) which divides the audio signal into three sub-bands directly, a set of filters (paragraphic equalization line) in each channel with dynamic adjustment of amplification/attenuation (AMP/ATT) of 10 dB (Fig. 10a, items *2–4*), and volume faders for each individual channel (Fig. 10a, item *5*). These are adjustable within the dynamic range from −30 to +30 dB.

The configurable architecture of the pre-equalizer (cross-filter, Fig. 10, item *1*) the AFR of which is shown in Fig. 11 allows the separation boundaries of bandpass channels to be adjusted. It also enables the signal in a given band to be amplified or attenuated, the filter type selected, and a rigid connection to be created between their boundaries. It also inverts channel polarities, thus resulting in attenuation of the signal in the intersection of frequency bands [9]. Paragraphic equalization blocks formed from a discrete set of bandpass filters perform an independent equalization in LF/MF/HF channels according to fader presets shown in Fig. 10a.

The laboratory application of the three-band crossover submodule in the media test mode is actually of practical interest when processing audio signals within specified frequency bands, its spectral routing, as well as when testing, calibrating, and correcting AFR of audio monitors [8].

In the case of the experimental electroacoustic analysis of signal shaping and correction of frequency-dynamic characteristics of audio channels at the output of the digital crossover submodule, the AFR of each equalization line filter is recorded (Fig. 10). Electroacoustic measurements are carried out on the basis of the automated laboratory bench (Fig. 12) controlled by the *RoomEQWizard* (*REW*)[6] software package consisting of the Behringer UMC404HD audio interface (with calibration script), the Behringer ECM8000 measuring microphone (with calibration file), and the Behringer K8 studio audio monitor.

[6] https://www.roomeqwizard.com/. Accessed December 02, 2022.

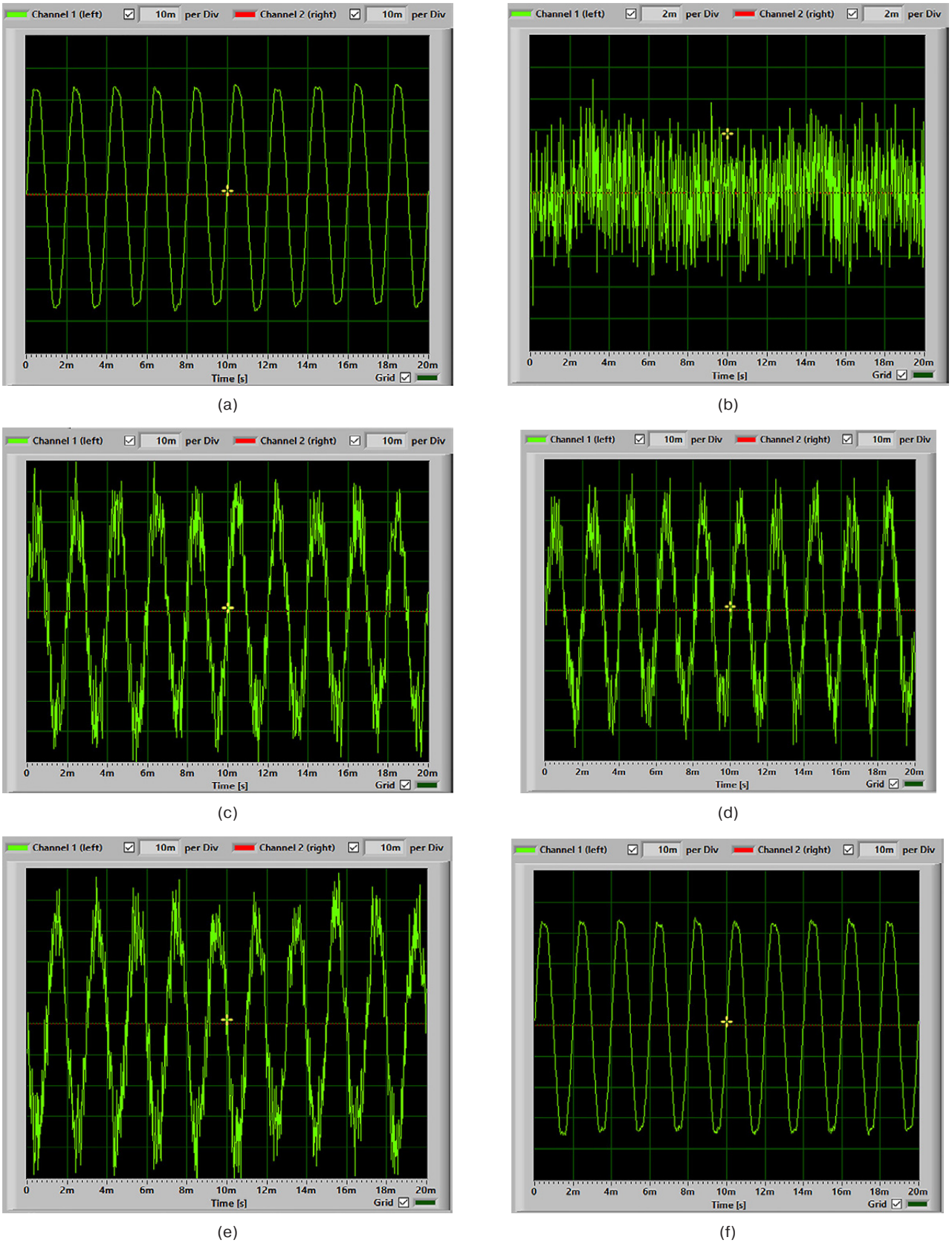

Fig. 9. Timing diagrams of the characteristics of the balanced audio path arranged according to the Di-Box/R Di-Box scheme:
(a) signal at balanced connection without induced noise; (b) additive noise; (c) signal at balanced connection with noise induced in the direct channel, SNR = 9 dB; (d) signal at balanced connection with noise induced in the inverted channel, SNR = 9 dB; (e) signal at unbalanced audio path connection and additive noise; (f) sum of direct and inverse (backward inverted) signal at R Di-Box, SNR = 35 dB

For reason of the purity of AFR measurements, the hardware presets of audio devices, architectural acoustics of the studio laboratory, as well as mutual positions between the measuring condenser microphone and audio monitor are not changed. Figure 13 shows the results of electroacoustic measurements of bandpass components at preset leveled value 0 dB for equalization crossover line filters, as well as at some fader position set arbitrarily (Fig. 10a, items *2–4*).

Controlling the presets of the equalization line allows the AFR of the audio monitor to be adjusted for specified characteristics of the frequency-dynamic balance at bandpass separation and audio signal panning (Fig. 14) [1]. In Figs. 13a and 13b, the AFR dynamic increase by 6 dB preset by the crossover is observed in the vicinity of 125 Hz frequency. A dynamic drop of 18 dB is observed in the region of 64 Hz. The dynamic increase in AFR by 12 dB at 800 Hz and the decrease in amplitude by 16 dB and 18 dB at 500 Hz and 1200 Hz, respectively, can be seen in Fig. 13d, as opposed to Fig. 13c. In the vicinity of 8 kHz frequency (Figs. 13d and 13e), a decrease in amplitude of 14 dB appears; while in the vicinity of 5 and 16 kHz, an increase of 16 dB occurs.

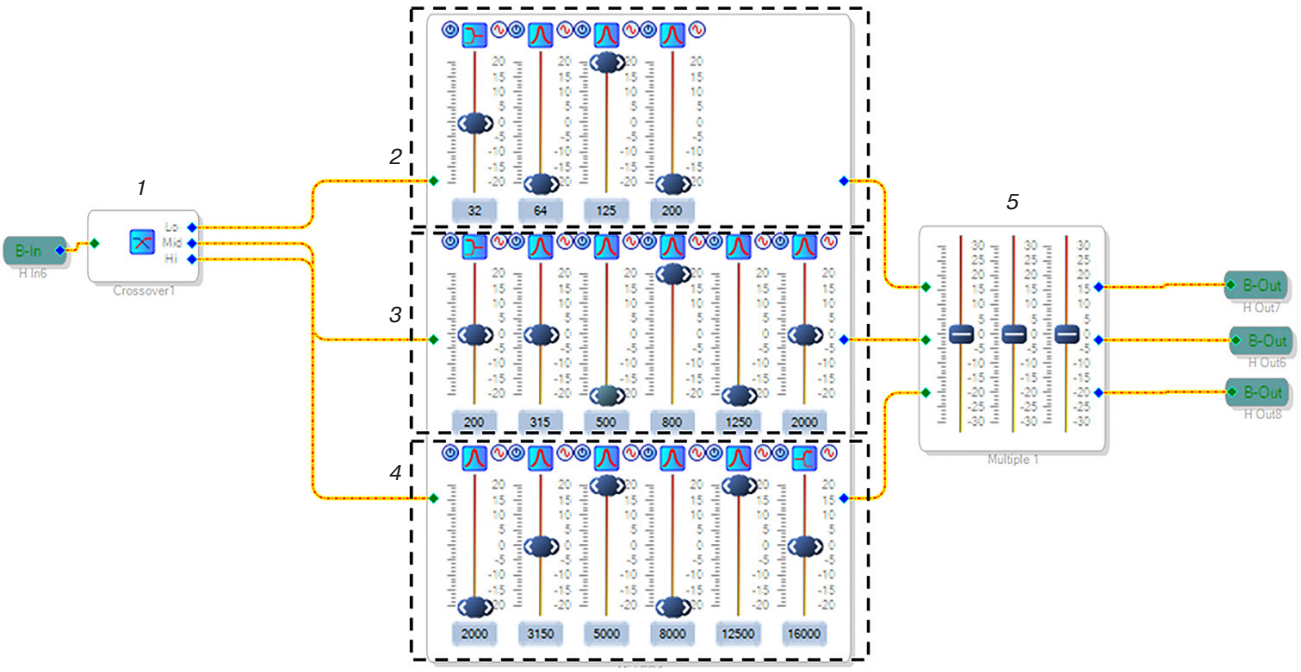

(a)

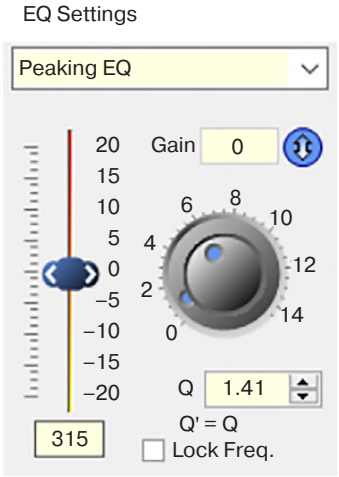

(b)

Fig. 10. Software-defined architecture of the three-band crossover submodule circuit:
(a) functional blocks:
1 is graphic pre-filtering equalizer;
2 is paragraphic LF equalizer;
3 is paragraphic MF equalizer;
4 is paragraphic HF equalizer;
5 is fader block for output volume control;
(b) parameterization of bandpass filter settings of the equalization block (frequency, goodness, limiting dynamic level of bandpass/notch AFR, AMP/ATT coefficient)

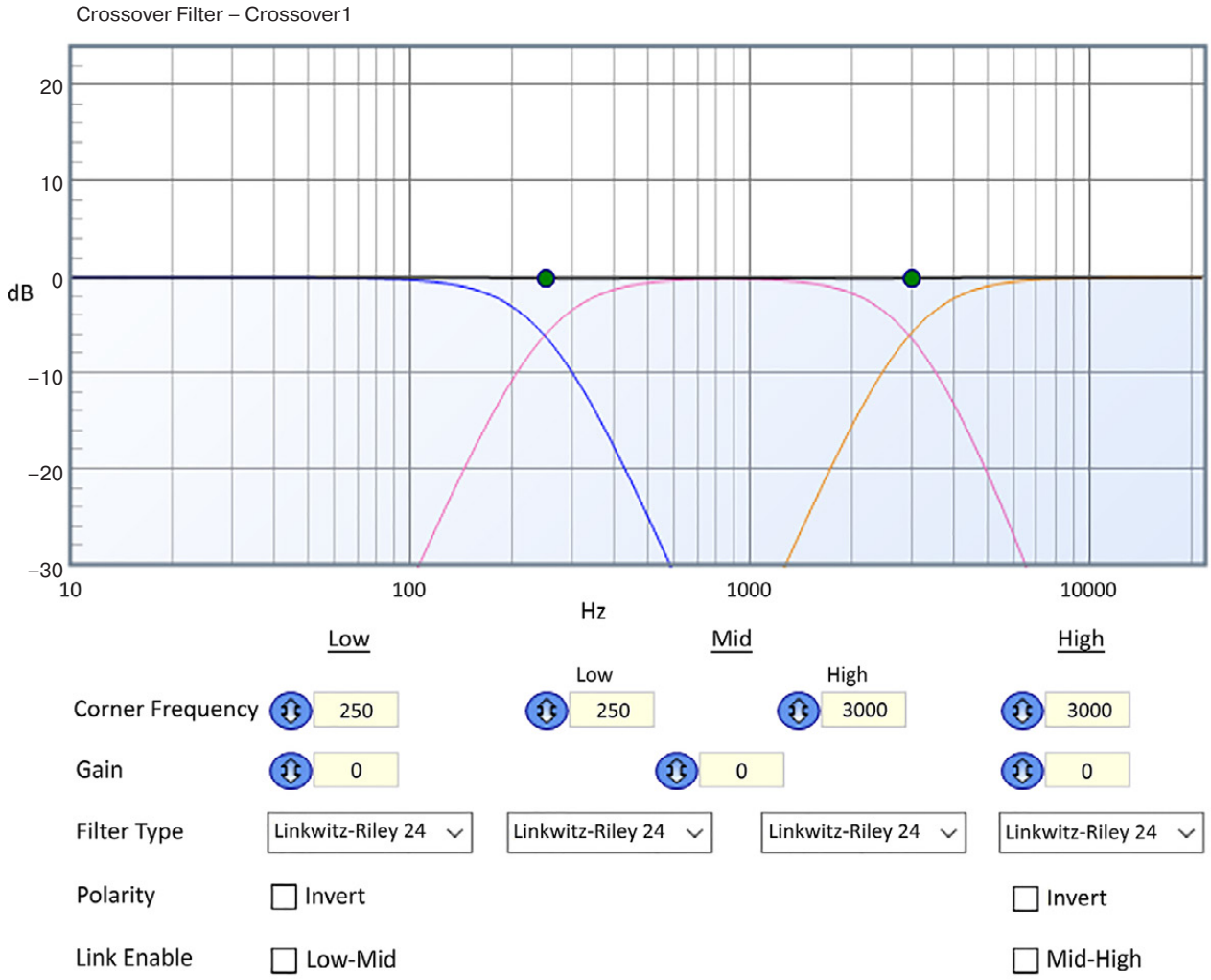

Fig. 11. Controlling the submodule settings of the digital three-band crossover digital crossover

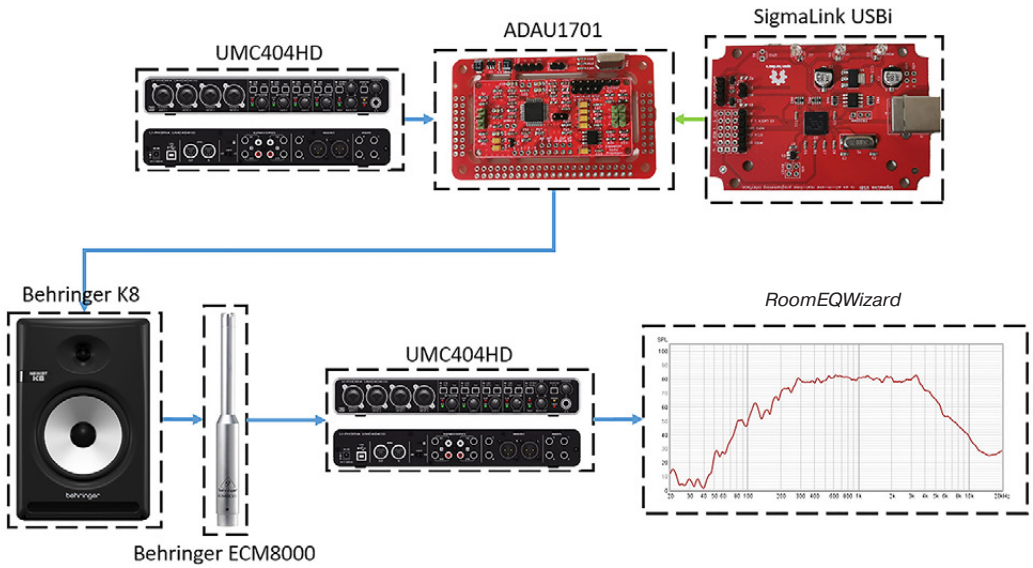

Fig. 12. Scheme of experimental research on controlling the AFR settings of a studio audio monitor using a digital crossover submodule

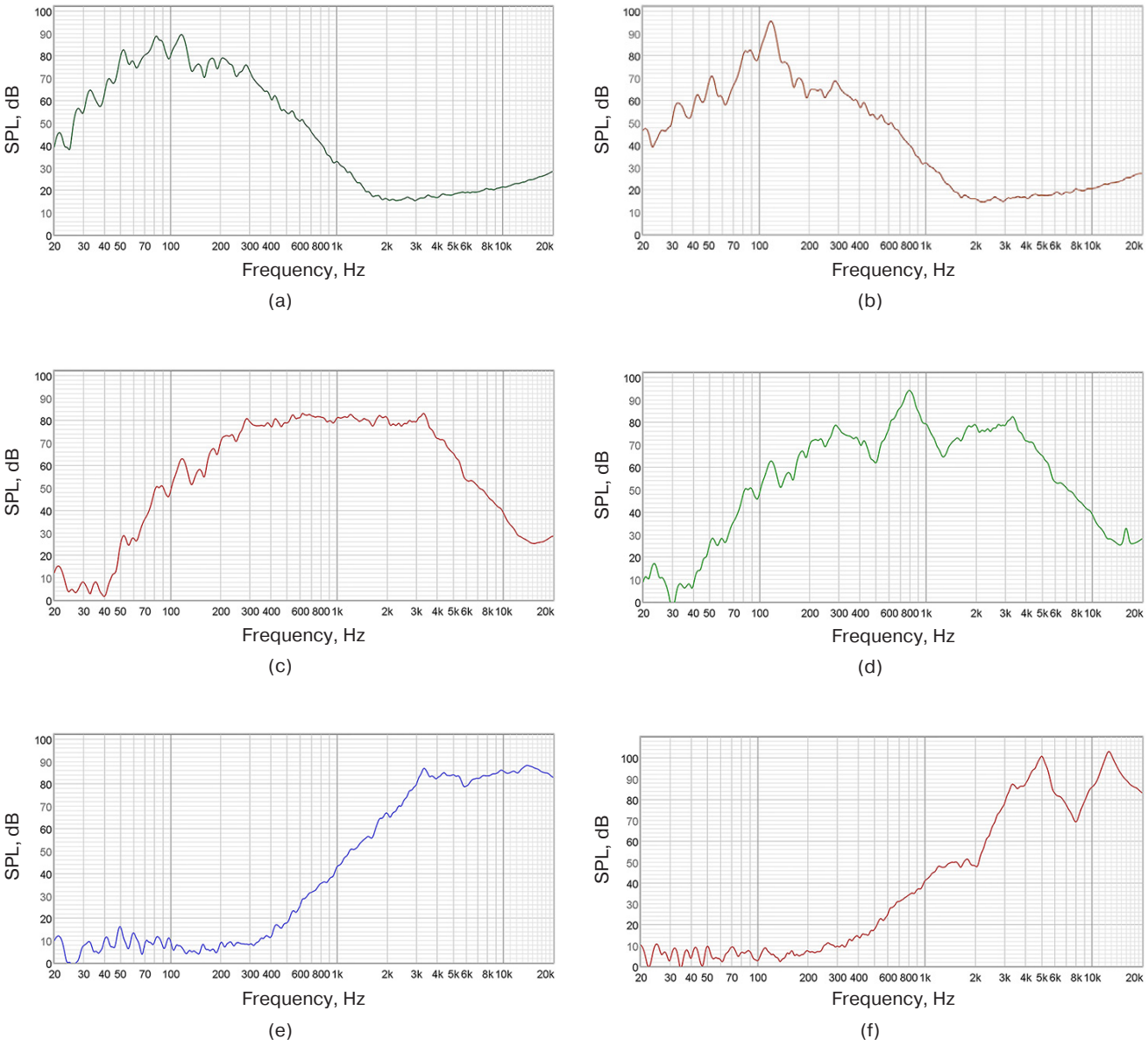

Fig. 13. AFR of the studio audio monitor formed by a digital crossover submodule in a given spectral region at preset leveled position 0 dB for filters (left) and arbitrary parameterization of the equalization line (right): (a), (b) LF audio channel; (c), (d) MF audio channel; (e), (f) HF audio channel

The measurements show that the three-way crossover submodule divides the audio signal into three audio-frequency channels: 20–250 Hz, 0.25–3 kHz, and 3–18 kHz. It also allows for repeatable AFR adjustment in each of them within the range from −30 dB up to 30 dB with the possibility of parametric correction. This allows this submodule to be used for audio signal routing in three-way loudspeaker systems, enabling independent research of each channel and panning the power spectral density function (PSDF) of the acoustic signal by frequency (Fig. 14).

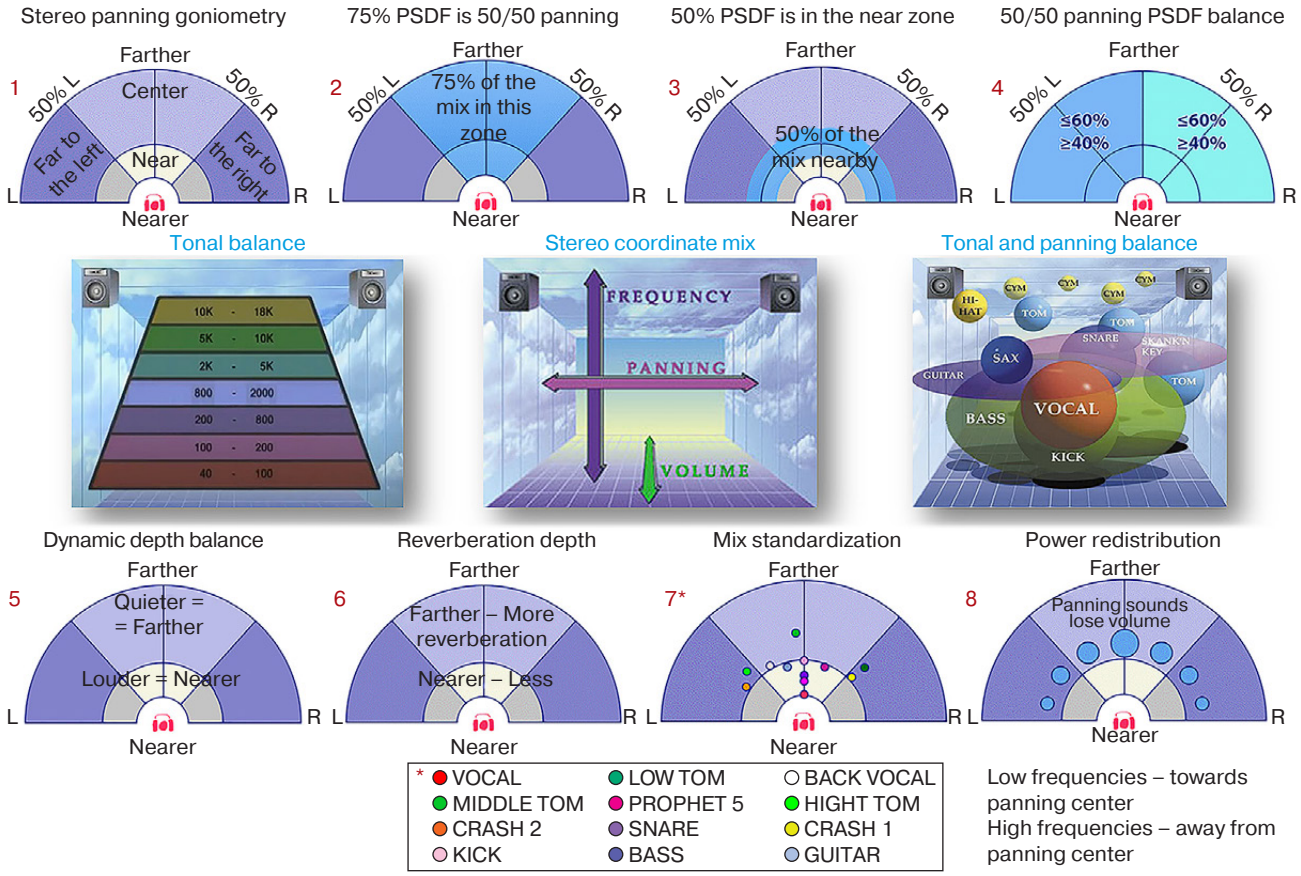

Fig. 14. PSDF panning by frequency (pitch) and sound intensity (depth)

3. ANALYZING THE COMPOSITE ARCHITECTURE CHARACTERISTICS FOR THE AUDIO EFFECTS SUBMODULE

The Effects audio effect submodule (Fig. 15) includes equalization, reverb, compression, and saturation blocks which form an insert line for audio signal processing. The audio mixer which admixes signals of the reverberator and saturator effects to the original audio signal (soundcheck) is installed at the submodule output with the ability to adjust the output levels of each of them. The digital architectural elements of the Effects submodule and its functional-graphical topology are shown in Fig. 15.

3.1. Analyzing and parameterizing the audio compressor characteristics

When analyzing the dynamic characteristics of the compressor which provides automated gain control in

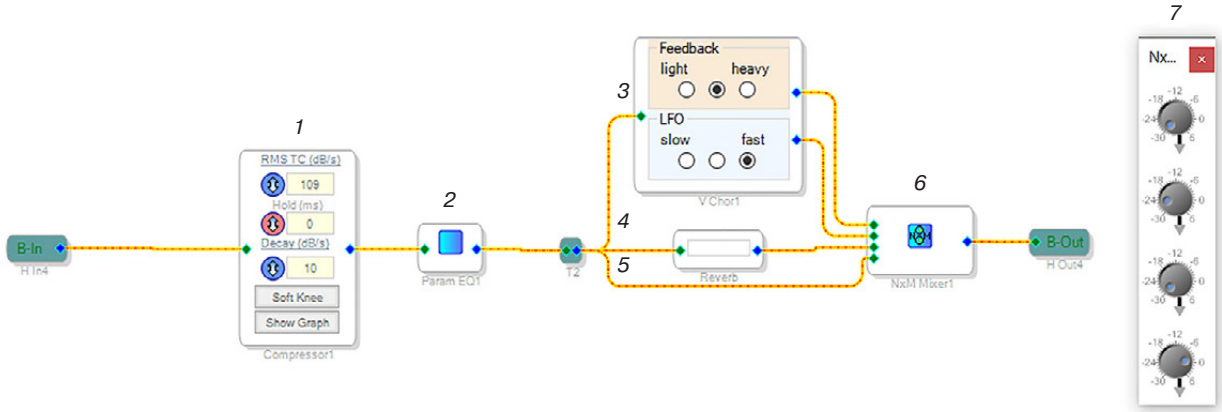

Fig. 15. Software-defined Box architecture of the audio effects submodule circuit: *1* is Compressor1; *2* is Param EQ1 parametric equalizer; *3* is V Chor1 saturation block; *4* is Reverb submodule; *5* is soundcheck signal route; *6* is 'N × M Mixer1' audio mixer; and *7* is 'N × M Mixer1' audio mixer adjustment window

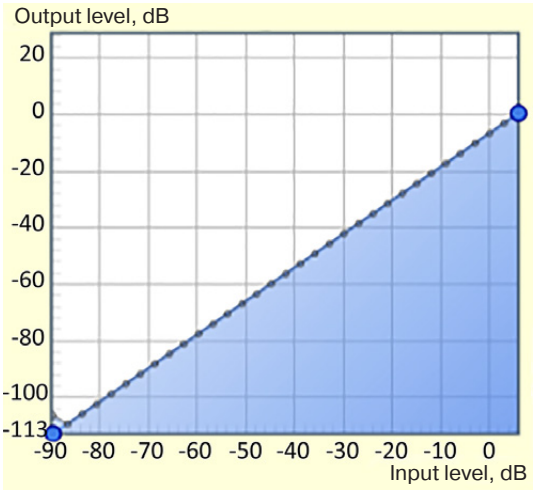

(a)

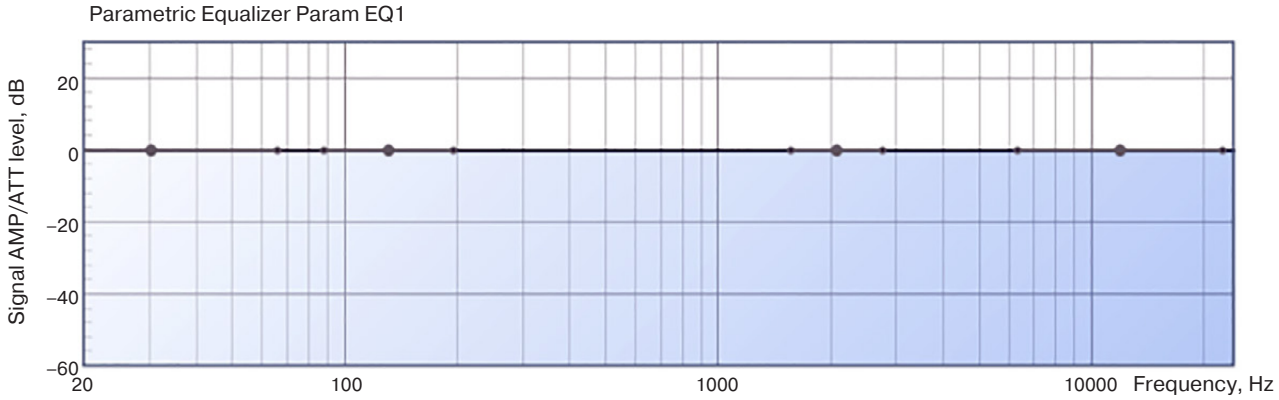

(b)

Fig. 16. Audio effects submodule presets: (a) initial amplitude response of the audio compressor (this mode does not affect the character of the test LFM signal passing); ▶ (b) equalization response of the submodule leveled at 0 dB ▼

the mode of equalizing the dynamic range of the digital submodule input signal, the level 0 dB needs to be set on the mixer for the channel with the signal bypassing the reverberator and saturator and minimum values for the rest. Figure 12 shows the experimental electroacoustic laboratory bench. It corresponds to the program switching of the audio module to the Effects submodule mode. Equalizer (Fig. 15, item *2*) is not involved, i.e. its AFR has a leveled zero dynamic value over the entire spectral band (Fig. 16). The submodule is tested using a monotonic linear-frequency modulated (LFM) signal of Sweep type within the range of 0.02–20 kHz and amplitude of 63 dB specified in the *RoomEQWizard* package.

The AFR of the audio monitor with free compression response is shown in Fig. 17. The signal level is −38.2 dB relative to full scale (dBFS). The AFR dynamic range is about 96 dB due to the roll-off in the LF region.

In order to evaluate the impact of the submodule compression response on the audio channel AFR, the graphic compressor presets may be changed by shifting the position of the compression response by 20 dB (Fig. 18).

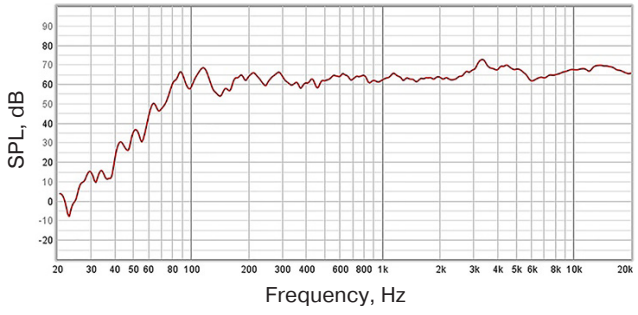

(a)

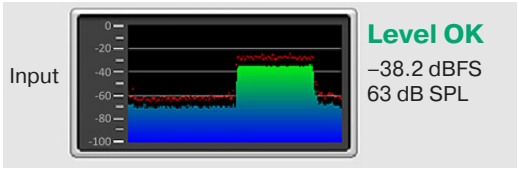

(b)

Fig. 17. Testing results for LFM signal of the audio path without compressor (reference AFR formation): (a) AFR of the audio monitor with free compression response (not subjected to the Effects submodule and compressor presets); (b) signal parameterization of *RoomEQWizard* presets (peak audio signal level relative to full scale in dBFS at the microphone)

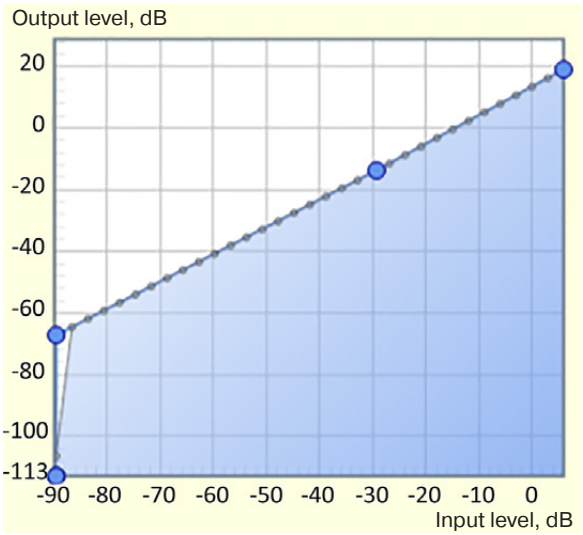

Fig. 18. Audio effects submodule presets: specified compression response with comparator threshold value of 20 dB (compander mode)

Figure 19 shows that the AFR level is increased by 25.7 dB including 5.7 dB of inherent noise in the audio channel. The AFR dynamic range of the audio monitors is 85 dB: i.e., 11 dB less than in the absence of any changes in the dynamic balance adjustment threshold.

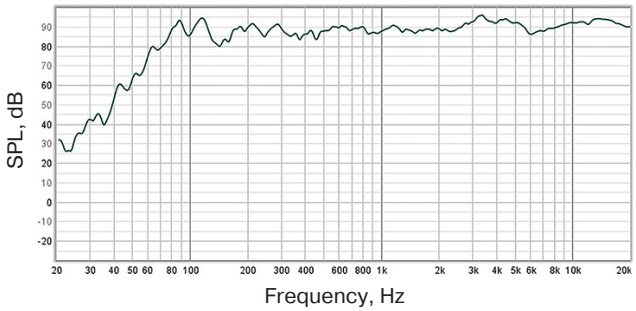

(a)

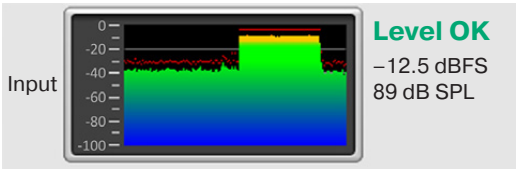

(b)

Fig. 19. Testing results for LFM signal of audio path with compressor at 20 dB threshold: (a) AFR of audio monitor with specified compression response; (b) signal parameterization of *RoomEQWizard* presets (peak audio signal level relative to full scale in dBFS at the microphone)

Next, in order to analyze the impact of the compressor on compressing the dynamic range of the audio channel, the output AFR level of the submodule is measured while setting the compressor response, in order to reduce the dynamic range of the input LFM signal to −18 dB as shown in Fig. 20.

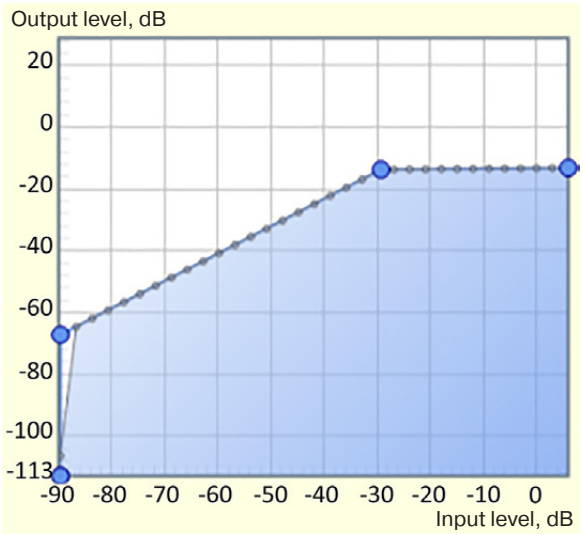

Fig. 20. Audio effects submodule presets: specified compression response with comparator triggering threshold −18 dB

The AFR shown in Fig. 21 indicates that the signal level has changed and is now −19.6 dBFS, i.e., increased by 18.6 dB relative to the uncompressed signal. The AFR dynamic range of audio monitors is 69 dB, i.e., 27 dB less than in the absence of any changes in the attenuation threshold.

Based on the electroacoustic measurement results, it can be concluded that the compressor allows the dynamic range of the signal to be compresses and its level increased over the whole frequency range according to the graphically defined compression response. It this way it stabilizes the dynamic range of the audio signal without distortion and overload of the tested audio device, and provides dynamic balance stabilization in the compander mode [10].

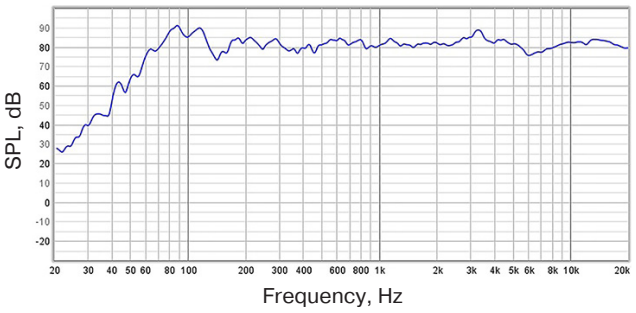

(a)

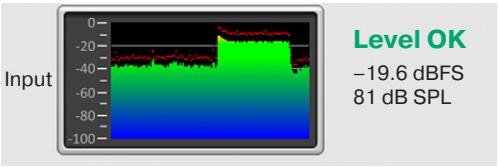

(b)

Fig. 21. Testing results for LFM signal of audio path with compressor at −18 dB threshold: (a) AFR of audio monitor with specified compression response; (b) signal parameterization of *RoomEQWizard* presets (peak audio signal level relative to full scale in dBFS at the microphone)

3.2. Analyzing and parameterizing equalizer characteristics

For the independent analysis of the equalization response of the Effects submodule, the compressor must be switched into bypass mode and the specified presets of the equalization filters (frequency, quality factor, and AMP/ATT) be set for the two options of forming the configuration of the acoustic signal AFR of the (Fig. 22). The paragraphic equalizer block of the multifunctional audio module allows up to 15 audio filtering elements to be set.

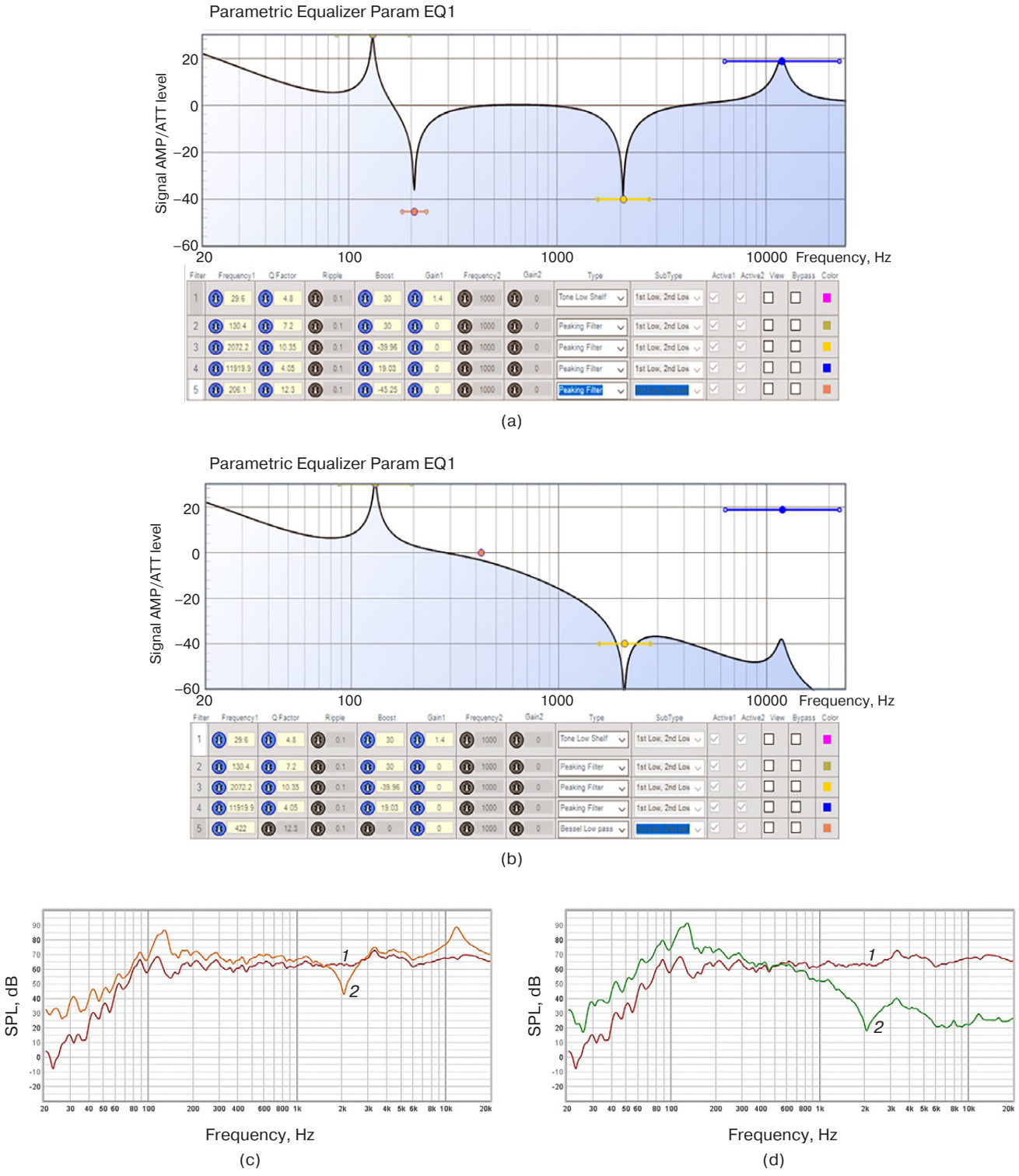

Fig. 22. Parameterization of the submodule equalization response for two options of filter configuration (a), (b) and corresponding electroacoustic AFR (c), (d) measured by microphone at the output of audio monitor (curves *1* are AFR without equalization, curves *2* are AFR after equalization)

As can be seen in Figs. 22b and 22d, the audio monitor AFRs repeat the preset equalization configurations (Figs. 22a and 22c) with a repeatability correlation of 0.85. This is due to the non-uniformity of the audio monitor AFR. In the section of the spectrum corresponding to the filter (Fig. 22a) at 130 Hz with 30 dB amplification, the amplitude is increased by about 20 dB, when compared to the amplitude of the same spectral band without processing. A similar situation can be observed for the filter at 2.072 kHz, with attenuation at −39.96 dB. Thus, the amplitude of the spectral band at this point is approximately 30 dB lower when compared to that of the original spectrum. A general dynamic rise can also be noted in the amplitude of the lower formants by an average of 20 dB, as set for the low-pass filter. Figure 22c shows that for the second option of equalization configuration, AFR with processing repeats the shape of the spectrum set on the equalizer (Fig. 22d). This can be established by an amplitude increase of 20 dB on average for frequencies in the range up to 100 Hz (in this case, the dynamic levels at frequencies "rolled-off" by physical parameters of the audio monitor are stretched), as well as by attenuation of high frequencies by about −35 dB.

Based on an analysis of the experimental characteristics, it can be concluded that the electro-acoustic AFR changes significantly depending on the equalizer settings, actually repeating the shape of the amplitude spectrum specified therein. This may be of practical interest when designing laboratory audio monitors with uniform AFR correction, as well as for testing media devices and acoustic systems when using a multifunctional module in this mode [11].

3.3. Developing and analyzing characteristics of a reverberator with timing architecture

Reverberation response is also analyzed in the independent activation of the graphic equalizer and the audio compressor submodule (Fig. 15, item *4*). A sequence of rectangular test pulses with an amplitude of 20 mV and controlled duty cycle generated by a specially developed VST plugin (synthesizer) in the visual-graphical system programming environment *Flowstone* (Fig. 23) is fed to the physical input of the ADAU1701 audio module through the UMC404HD audio interface [1]. The reverberator characteristics were analyzed on the basis of the electro-acoustic measurement laboratory bench as shown in Fig. 8.

In the proposed submodule architecture with timing reverberation [12] (Fig. 24), the signal passes through: the low-pass filter (item *5*) with a cutoff frequency of 6 kHz; the 21.25 ms digital delay block (item *6*) in 1020 samples; and the feedback loop (item *4*) providing control over 1–3 s timed reverberation. The feedback loop has two delay elements (item *6*) with a delay of 4 samples, and one with a delay of 12 samples with the ability to adjust the level of the passing signal. The delayed signal passes to the output in parallel with the original signal. This is reduced in frequency by a factor of 4 when compared to the sampling frequency of the system.

The results of the reverberation audio channel characteristic of the digital submodule with timing architecture are in the form of oscillograms recorded using the *Soundcard Oscilloscope* and the UMC404HD audio interface. This enables the impact of the specified time delays to be evaluated. The transfer factor and feedback

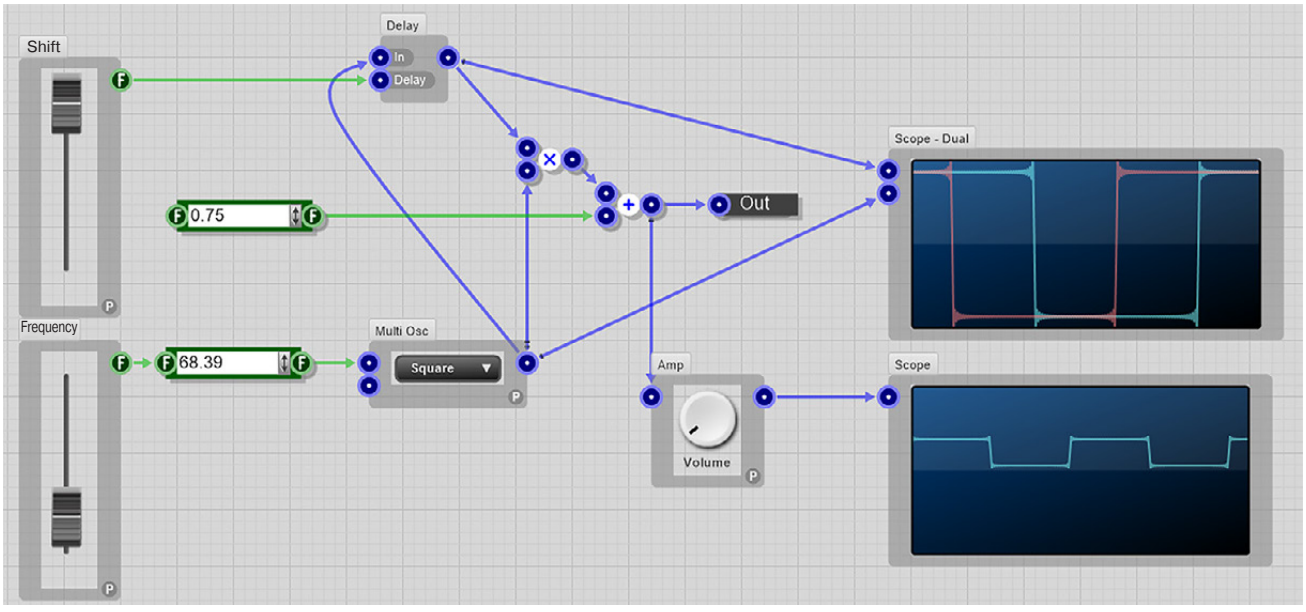

Fig. 23. VST synthesizer of test rectangular pulses

loop attenuation for generating echo reverberation signals are shown in Fig. 25.

Ananalysis of the characteristics obtained shows the amplitude instability of the test rectangular pulses: up to 5 mV due to the presence of a differential circuit at the UMC404HD audio interface output. In addition, the inherent noise of the sound card and ADSP module of about −40 dB is admixed to the signal. The oscillogram shown in Fig. 25b demonstrates that at given parameters of the reverberation limit level (0 dB for the delayed source signal, −8 dB for the feedback line (Fig. 24, item *2*), and −10 dB for the volume fader of the additional delay (Fig. 24, item *8*)), the main signal copies delayed by 500 ms and 1s with amplitudes of 3.5 mV and 1.0 mV, respectively, are added to the 12.5 mV main signal. When the signal is attenuated by −10 dB, the amplitude of the original signal (Fig. 25c) in the reverberation circuit is equal to 17 mV. Of the fragmentary components, only the first one with an amplitude equal to 2 mV remains. At the same time, at minimum parameters of feedback level (Fig. 25d) (−14 dB to the feedback circuit (Fig. 24, item *2*)), the amplitude of the original signal is equal to 17 mV. Of the additional components only the first one with an amplitude equal to 4 mV remains.

Thus, a timing-controlled digital reverb block adds delayed copies to the original audio signal. This submodule enables the feedback depth and its admixing degree to the original signal to be adjusted, i.e. used for simulating characteristics of the diffuse vector field of architectural acoustics. It is of interest in the creation of phantom reverberation effects, as well as when studying the properties of the audio signal and its qualitative reproduction under given conditions of the propagation environment [13].

3.4. Analyzing and parameterizing the signal saturator characteristics

The characteristics of V Chor1 saturation block of the Effects submodule (Fig. 15, item *3*) are analyzed and parameterized using a sinusoidal signal in the spectral region. The built-in low-frequency oscillation (LFO) add-on determines the delay time modulated by the low-frequency oscillator. It has three modes of operation: Slow (i.e., with the longest delay); Normal (medium); and Fast (i.e., with the shortest delay). The Feedback add-on defines the degree of mixing the delayed signal with the original one: Light (i.e., a small part is admixed); Normal (medium); and Heavy (oversaturated). The signal saturation mode in the Effects submodule is of practical interest in developing and testing digital media devices which enable the original signal (soundcheck) to be saturated with odd formants simulating the nonlinear distortion effect of transistor stages of analog audio tracts [4]. The saturation block consists of the positive feedback circuit and a low-frequency delay time modulator. The mode settings in the circuit are controlled by the 'N × M Mixer1' volume mixer at the submodule output (Fig. 15, item *7*).

The spectral response characteristics shown in Fig. 26 indicate that saturation adds multiple odd subharmonics to the spectrum of the test (original) signal with a frequency of 1 kHz. The spectrum analyzer has the maximum value hold mode enabled. In this way, the spectrum snapshot is taken one minute after the submodule starts operating. The results of analyzing the saturator response are given in the table.

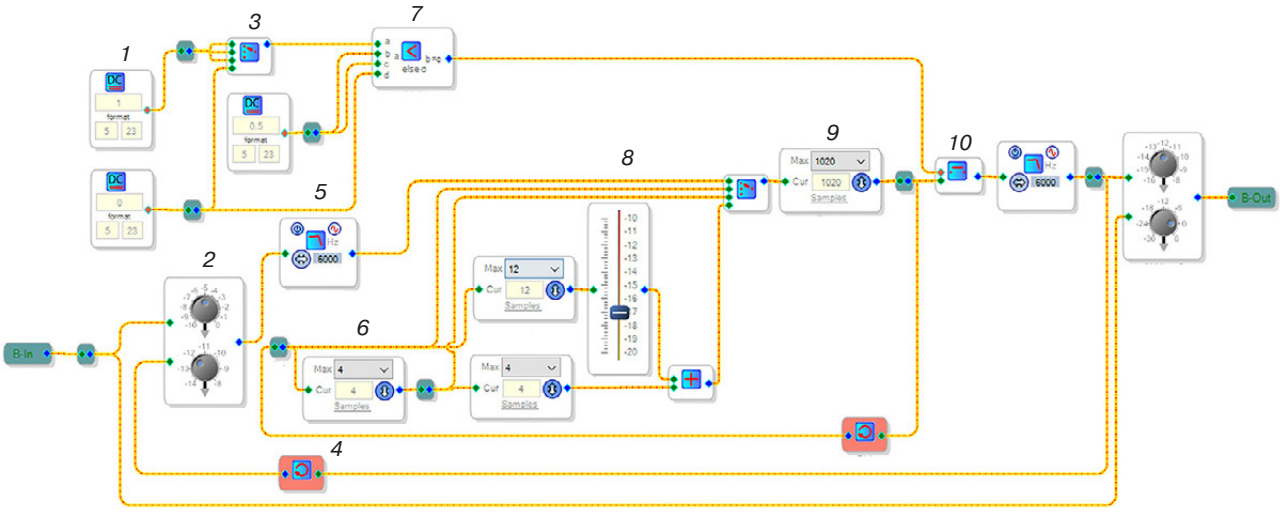

Fig. 24. Software-defined architecture of the 4th order timing reverberator submodule circuit:
1 is constant value generation blocks; *2* is mixer determining the feedback depth; *3* is synchronous multiplexer; *4* is feedback creation block; *5* is low-pass filter; *6* is signal delay block; *7* is comparator; *8* is additional delay fader; *9* is main signal delay block; *10* is digital key

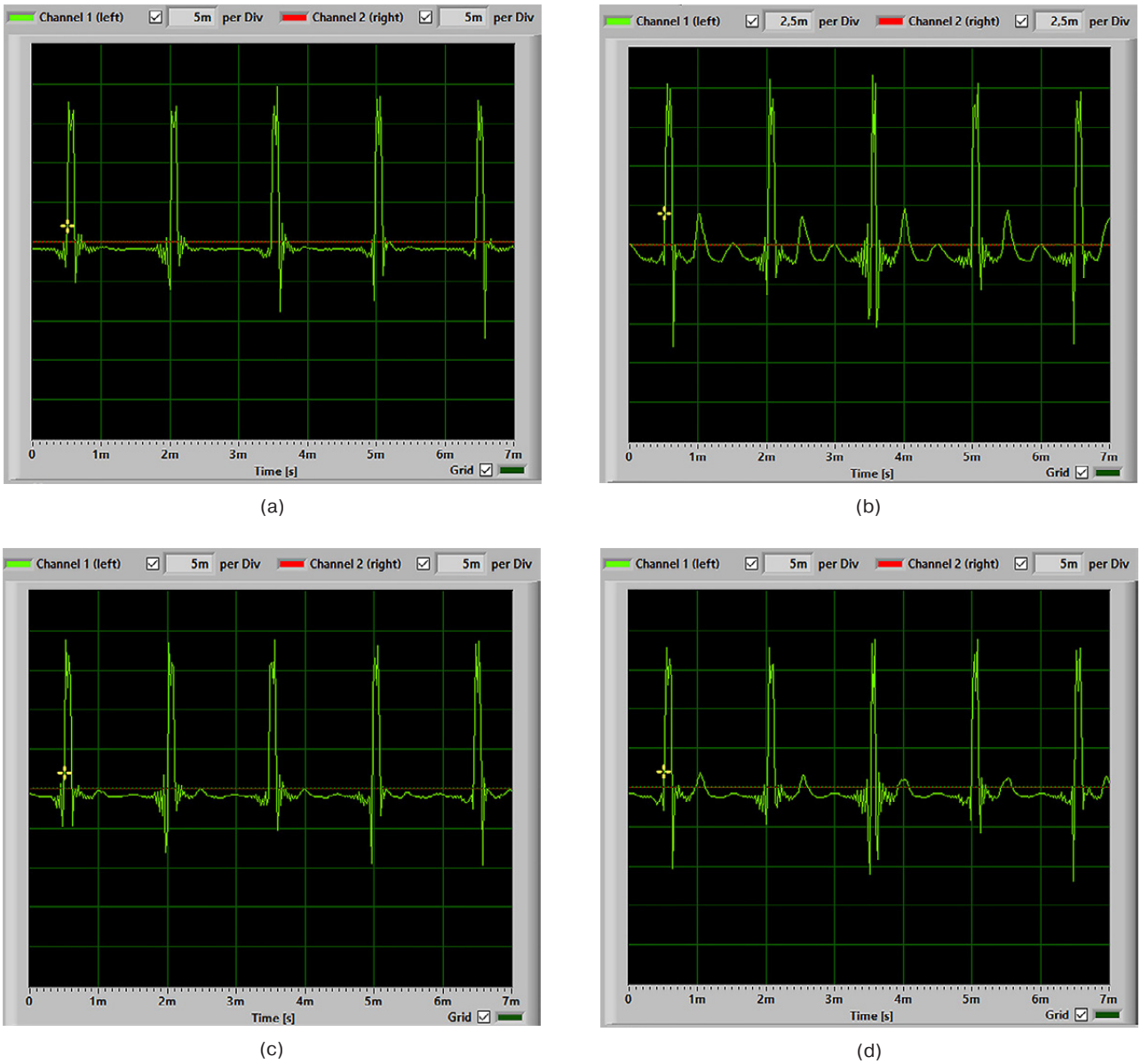

Fig. 25. Oscillograms of studying reverberation audio channel response: (a) test pulse signal; (b) audio signal with the limiting reverberation level corresponding to the circuit presets (Fig. 24); (c) audio signal attenuated by −10 dB in the reverberation circuit; (d) signal with the minimum feedback level corresponding to the circuit presets (Fig. 24)

Table. Experimental characteristics of the saturator at given add-ons

Saturator add-on (operation mode)	Feedback–Light	Feedback–Heavy	LFO–Slow	LFO–Fast	Feedback–Light, LFO–Slow	Feedback–Heavy, LFO–Fast
Amplitude of test signal with frequency 1 kHz, mV	60	60	60	60	60	60
Amplitude of the 1st subharmonic, mV	15	15	15	18	17	20
Amplitude of the 2nd subharmonic, mV	7	5	6	8	9	11
Frequency bandwidth carrier at 5 mV level, Hz	200	100	100	50	200	50
Number of subharmonics with a level of at least 1 mV	6	5	5	5	9	8

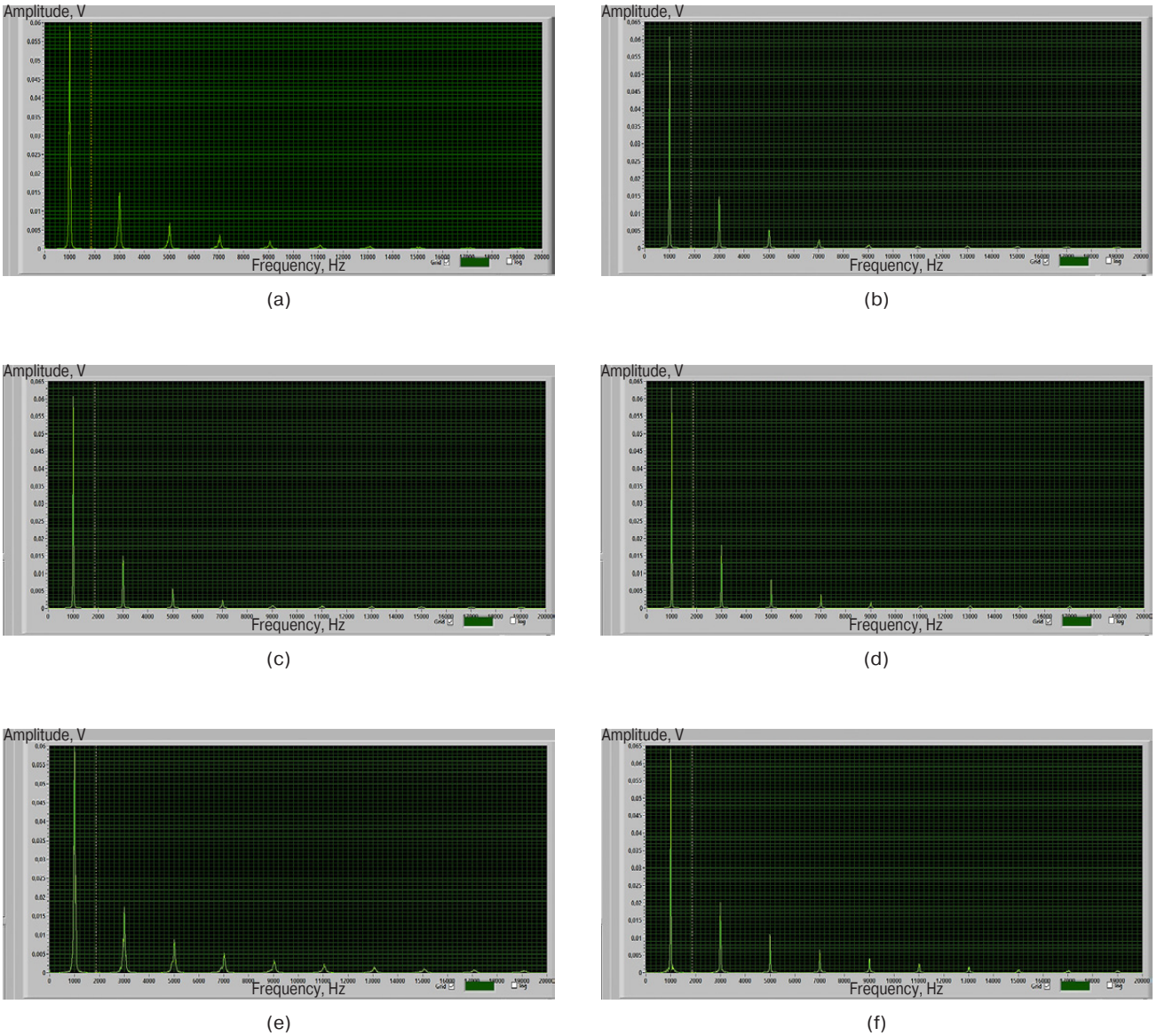

Fig. 26. Spectrograms of the signal saturation mode:
(a) output signal with the Feedback–Light add-on set;
(b) output signal with the Feedback–Heavy add-on set;
(c) output signal with the LFO–Slow add-on set;
(d) output signal with the LFO–Fast add-on set;
(e) output signal with the Feedback–Light and LFO–Slow add-ons;
and (f) output signal with the Feedback–Heavy and LFO–Fast add-ons

The data in the table indicates that the saturator operation in the Feedback–Light and LFO–Slow combined mode produces the largest number of subharmonics and the largest bandwidth of the original signal. The Feedback–Heavy and LFO–Fast mode yields the largest amplitude of the carrier and the first two subharmonics, and the smallest generated frequency bandwidth at 5 mV. Thus, the saturation block adds odd harmonics to the spectrum of the original signal, thus widening the formant band and increasing the spectral power density of the signal. Additionally, the number of subharmonics and their amplitude can be adjusted. The signal saturation mode enables effects of phono-tertial/phono-octave polyphony to be created. These are often used in processing real-time audio signals including electroacoustic measurements when analyzing the intensity distribution of spectrally saturated diffuse sound field [14].

4. DEVELOPING, ANALYZING AND EVALUATING THE EFFICIENCY OF THE AFR AUTOCORRECTION SUBMODULE

Due to their nonuniformity, the phase-dynamic responses of audio monitors, as well as AFR of the diffuse space of sound field propagation (including those caused by wave dispersion) are usually corrected by applying compensation filters to the distorted parts of AFR [4]. AFR uniformity is extremely important for correct audio signal processing and electroacoustic measurements. The architecture for the AFR autocorrection circuit, as proposed in this paper, enables the frequency-dynamic and phase balance of the speakers to be equalized. This is due to the specific features of AFR nonuniformity of the diffuse space, for example, a recording studio [12]. In order to create an adaptive filter in the circuit of the AFR autocorrection submodule, the AutoEQ developed block is used. This enables a corrective chain of matched filters to be automatically built, according to the AFR numerical values loaded into it.

Figure 27 shows an experimental scheme for synthesizing the adaptive parameterization and measurement of multifunctional audio module characteristics in the AFR autocorrection mode. The Behringer ECM8000 measuring microphone is installed opposite the center of the audio monitor speaker at an axial distance at the specified recording point. This is so that the sound pressure level (SPL) is no lower than 75 dB, while the audio module is included in the audio path between the output of the audio interface and the input of the active studio monitor.

The procedure for AFR monitor autocorrection consists in measuring the diffuse space AFR and creating a counterbalanced adaptive AFR of the correction filter. This enables the dynamic range of the electroacoustic path to be leveled within the limit range of ±10–15 dB due to phase-dynamic compensation in a given volume of the sound field [8]. In the *RoomEQWizard* package, a test LFM signal of the Sweep type in the 0.02–20 kHz bandwidth is generated at the audio interface output. Based on the data obtained by the program from the Behringer ECM8000 measuring microphone (AFR of the microphone and the audio interface is compensated by a calibration file), the acoustic AFR/PFR (phase-frequency response) of the room is created. This integrates the AFR/PFR of the signal audio path including studio audio monitors (Fig. 28a) which can then be exported from the program as a data array (frequency, amplitude, and phase) in ".txt" format (Fig. 28b).

Loading this file into *SigmaStudio* requires the header inside the export file to be changed, as shown in Fig. 28c. Next, the export file is loaded into the AutoEQ block of the AutoCorrection submodule. The AFR for the adaptive filtering system is automatically calculated and plotted (Fig. 29a).

The block interface enables the number of filters (up to 15) to be selected, along with the manual preset/adjustment of their parameters. The experimental curves of AFR autocorrection results generated by the AutoCorrection submodule are shown in Fig. 29b. The limit deviation of the dynamic range after autocorrection is within ±10 dB in the region up to 100 Hz and ±5 dB in the 0.1–20 kHz band. Auto-measurement mode and data file loading into ADAU1701 audio processor is provided for the different conditions of auto-compensation for AFR nonuniformity of the diffuse space due to correction of AFR of audio monitors.

The curves shown in Fig. 29b indicate that autocorrection allows the dynamic level "roll-off" in the band below 80 Hz to be raised by almost 40 dB. It also enables the average signal level in the dip region to be raised, e.g., by about 7 dB at 1 kHz without affecting peak values, e.g., at 80 Hz and 3.3 kHz. AFR non-uniformity in the measurements presented herein is ±10 dB in the region up to 100 Hz and ±5 dB in the 0.1–20 kHz band. This makes the AFR of the diffuse space in some volume of the sound field relatively uniform during electroacoustic tuning of studios and halls. This enables media systems to be tested, and audio equipment to be tuned and adjusted without introducing distortion [12].

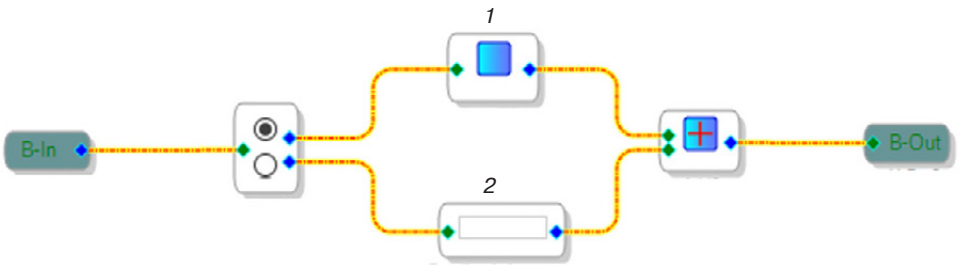

Fig. 27. Software-defined architecture of the AFR autocorrection submodule circuit: *1* is AFR autocorrection block Auto EQ1; *2* is Feedback Attenuator submodule for suppressing positive feedback automatically

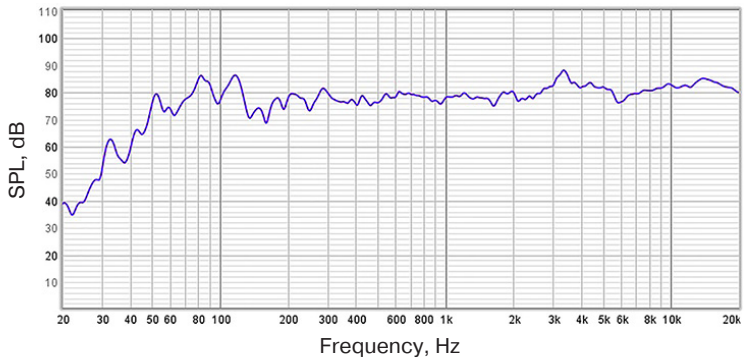

(a)

```
* Measurement data measured by REW V5.20.9
* Source: ASIO UMC ASIO Driver, In 1
* Format: 256k Log Swept Sine, 1 sweep at -12,0 dBFS with no timing reference
* Dated: 07.12.2022 15:57:29
* REW Settings:
*  C-weighting compensation: Off
*  Target level: 75.0 dB
* Note:
* Measurement: Dec 7
* Smoothing: None
* Frequency Step: 1/24 octave
* Start Frequency: 1.000 Hz
*
* Freq(Hz), SPL(dB), Phase(degrees)
1.000000, 34.963, -124.7207
1.030000, 34.536, -124.7025
...
...
...
19000.000000, 81.612, 19.5586
19500.000000, 80.173, 22.6615
```

(b)

```
"Sensitivity Excess Phase - dB SPL/watt (8 ohms, @0.50 meters) (High)"
        "Hz"  "Mag (dB)"       "deg"
1.000000, 34.963, -124.7207
1.030000, 34.536, -124.7025
...
...
...
19000.000000, 81.612, 19.5586
19500.000000, 80.173, 22.6615
```

(c)

Fig. 28. AFR of diffuse space:
(a) at an arbitrary point of sound field distribution of the laboratory studio for signal radioacoustics, audiovisual systems, and technologies of the Department of Radio Wave Processes and Technologies at MIREA – Russian Technological University (RTU MIREA);
(b) exported AFR/PFD data array corresponding to the curve in (a); and
(c) correction of the data export format from the *RoomEQWizard* package to the *SigmaStudio* environment

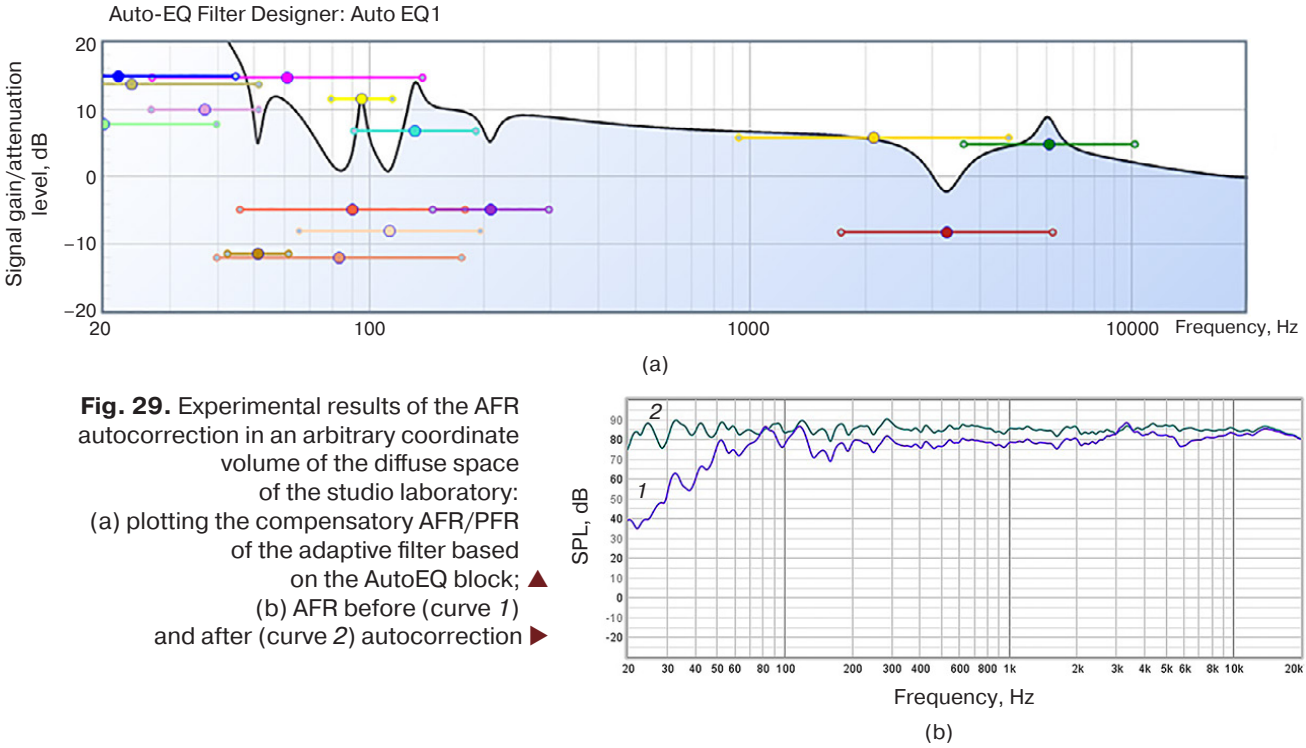

Fig. 29. Experimental results of the AFR autocorrection in an arbitrary coordinate volume of the diffuse space of the studio laboratory: (a) plotting the compensatory AFR/PFR of the adaptive filter based on the AutoEQ block; ▲ (b) AFR before (curve *1*) and after (curve *2*) autocorrection ▶

5. DEVELOPMENT AND SIGNAL-PARAMETRIC ANALYSIS OF THE AUTO-COMPENSATION SUBMODULE OF ELECTROACOUSTIC POSITIVE FEEDBACK

Electroacoustic positive feedback phenomenon is known to result in autogeneration, caused by the formation of a mode of sharply increasing phase-amplitude balance between the microphone and the audio monitor speaker. This is in the strict sense, determined by conditions of the sound propagation medium, the distance between the sound source and receiver, as well as their resonant frequencies and directional diagrams. The source thereof is the inherent noise of the electroacoustic channel [5]. Electroacoustic positive feedback is suppressed by disturbing the phase-dynamic balance of the system by means of initiating the selective phase drift (rendered phase shifting of the signal at critical resonant frequencies) or creating narrow-band notch filtering (dynamic suppression of the signal at critical frequencies) [15]. Figure 30 shows the submodule connection circuit for auto-compensating the electroacoustic positive feedback. In this case, the low position should be selected on the '1 × N − 3' switch in the auto-correction submodule, corresponding to the mode of auto suppression of acoustic positive feedback in the Auto EQ1 Box submodule.

As shown in Fig. 31, the experimental scheme of the laboratory research of the audio module in the positive feedback auto-compensation mode requires the following audio channel routing: the audio signal induced into the diffuse space by the audio path inherent noise within the range from −50 to −40 dB from the monitor goes from the Behringer ECM8000 measuring microphone to the ADAU1701 input. From here it passes through the Auto EQ1 positive feedback auto-compensation submodule scheme. The signal is then routed to the input of the UMC404HD audio interface. From the output it goes to the Behringer K8 audio monitor. The microphone is located in the main line of the directional pattern of the audio monitor speaker at a distance of 1m. The audio interface input is set to sensitivity of 10 dB, in order to ensure the microphone picks up the inherent noise of the electroacoustic channel.

The initiated frequency resonances are compensated (notched) using the Auto EQ1 submodule included in the audio path. Then the selectively attenuated signals are fed to the audio interface input, where the oscillogram is recorded using the *Soundcard Oscilloscope*.

The software-defined circuit configuration of the positive feedback auto-compensation notch submodule (Fig. 32) is a system consisting of 18 auto-filtering blocks connected in series. This system enables selection at a nominally specified frequency combination of 31, 63, 87, 125, 175, 250, 350, 500, 700 Hz and 1, 1.4, 2, 2.8, 4, 5.6, 8, 11.2, 16 kHz with controllable bands providing an overlapping frequency range of 0.02–18 kHz [15].

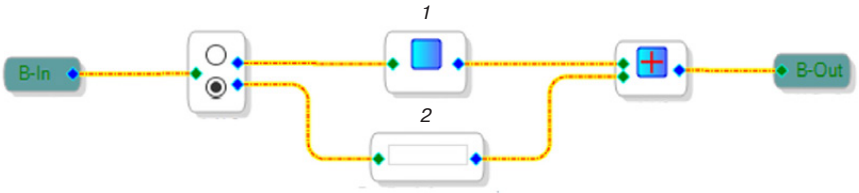

Fig. 30. Software-defined architecture of the submodule connection circuit for auto suppression of acoustic positive feedback: *1* is the AFR auto correction block Auto EQ1; *2* is the Feedback Attenuator submodule of automatic positive feedback suppression

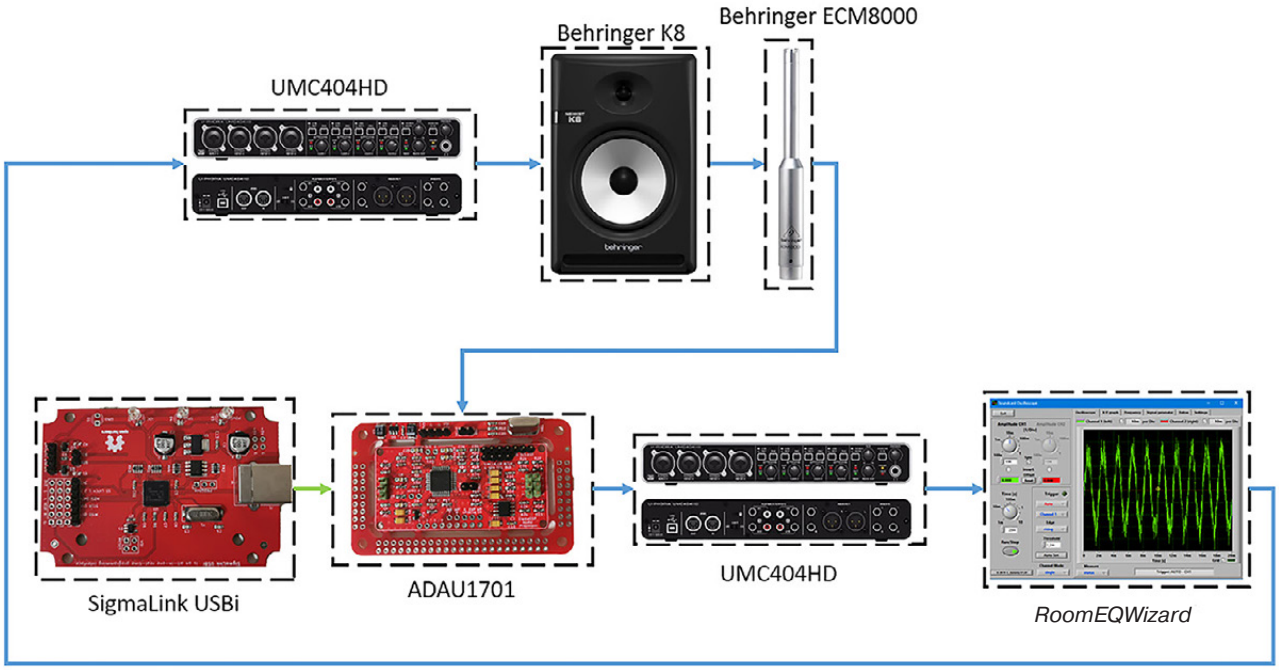

Fig. 31. Scheme of the experimental research of the multifunctional ADSP module in the mode of switching the submodule of electroacoustic positive feedback auto-compensation on

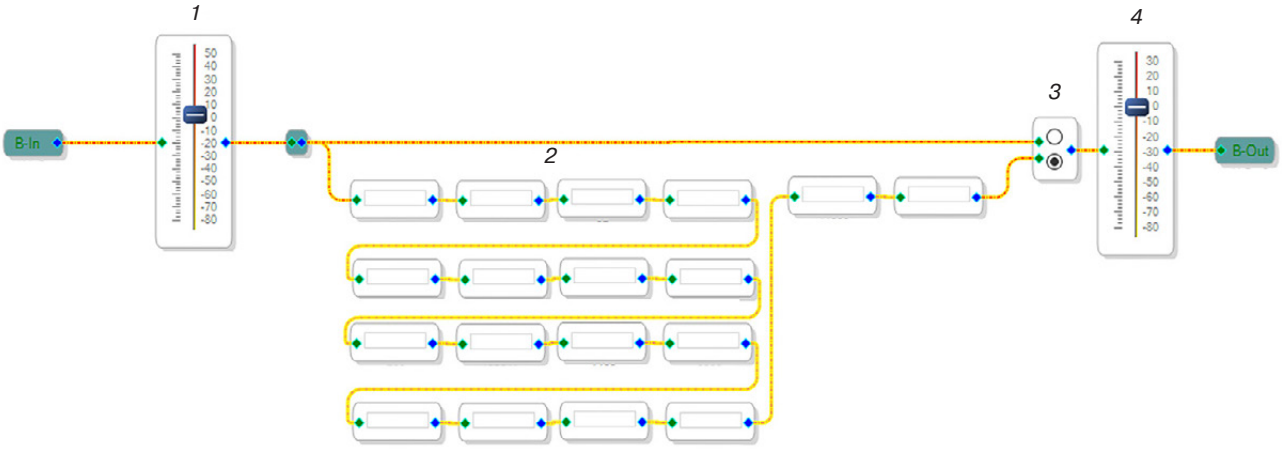

Fig. 32. Software-defined architecture of the circuit for positive feedback auto-compensation submodule: *1* is Single 1_2 input volume fader; *2* is the line of notch filters; *3* is 'N × 1 – 1_2' digital switch; *4* is the Single 2_2 output volume fader

frequency at the adjustable level of notch attenuation of the signal within the range from 0 dB to −100 dB.

In this method of positive feedback notch auto-compensation, notch filters are triggered only when resonance occurs and after the user-defined time of 0–10 s. Then they are reset, thus preventing the system from significantly impacting the AFR of the speaker. The filter frequencies and goodness (Fig. 33, item *6* and *7*) fully overlap the entire operating frequency range of 0.02–20 kHz at the input dynamic range from −50 to 80 dB.

When examining the Auto EQ1 submodule, a test signal in the form of the audio channel inherent noise with the level from −50 to −40 dB is formed at the circuit input. Figure 34 shows the experimental spectral-time characteristics of the signal auto-compensation of the electroacoustic positive feedback. This illustrates the mode of selective suppression of the initiated frequency-resonance spikes up to the level of 2.75 mV (below the dynamic level of the audio path inherent noise). The microphone continues to pick up the useful audio signal and noise at any other frequencies, including spectral formants which do not fall into the unstable mode region of the system. If the resonance does not occur within 10 s, the notch filter is switched off, thus preventing AFR notch distortion caused by random (simultaneous) resonances. The submodule of the electroacoustic positive feedback notch auto-compensation is of practical interest when testing studio media systems for stability according to the Nyquist criterion [4]. It also prevents overloading of audio monitors due to the electroacoustic positive feedback effect. When analyzing the frequency-time characteristics shown in Figs. 34a and 34b, special attention should be paid to the presence of a periodic signal with an amplitude of 240 mV consisting of 7 harmonic components with a level higher than 10 mV. The characteristics shown in Figs. 34c and 34d demonstrate the presence only of a noise signal with an amplitude of 2.75 mV without pronounced frequency components.

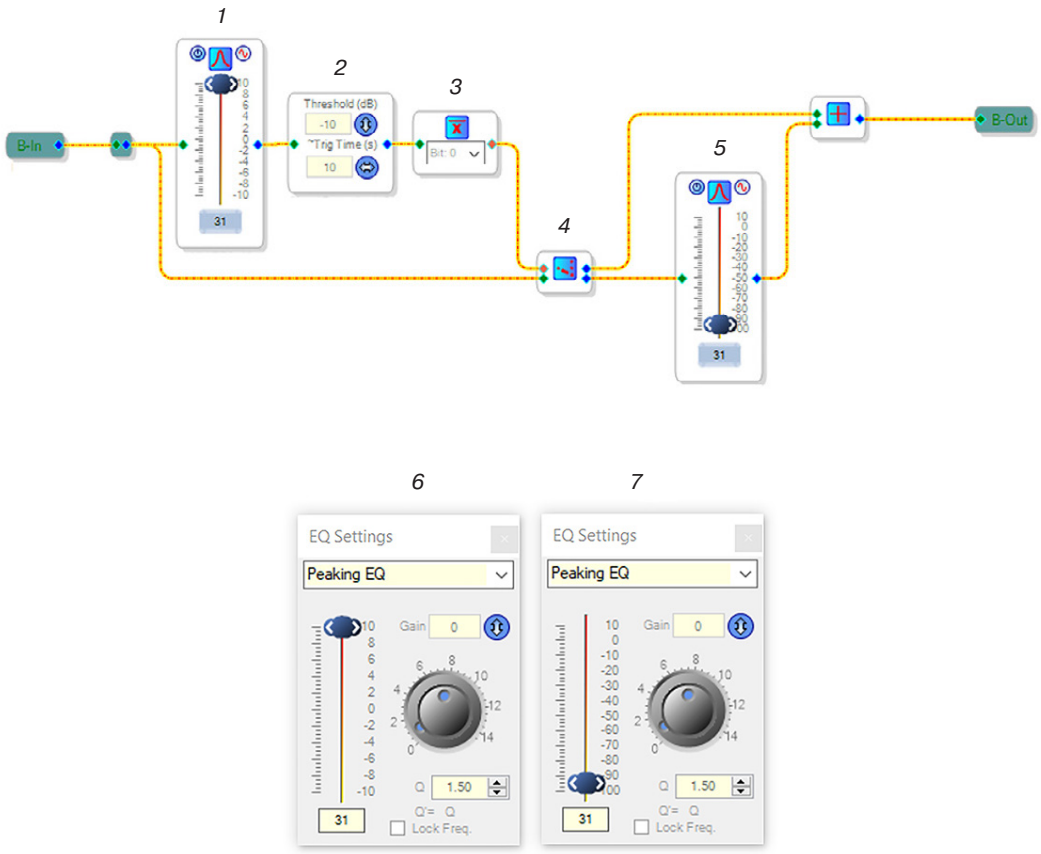

Fig. 33. Scheme of the block of bandpass auto-tracking the acoustic positive feedback: *1* is Mid EQ3_19 BF; *2* is Signal Detection1_21 block; *3* is ZeroComp1_21 zero-comparison block; *4* is DmX2_19 demultiplexer; *5* is Mid EQ2_21 NF; *6* is Mid EQ3_19 BF adjustment window; and *7* is Mid EQ2_21 NF adjustment window

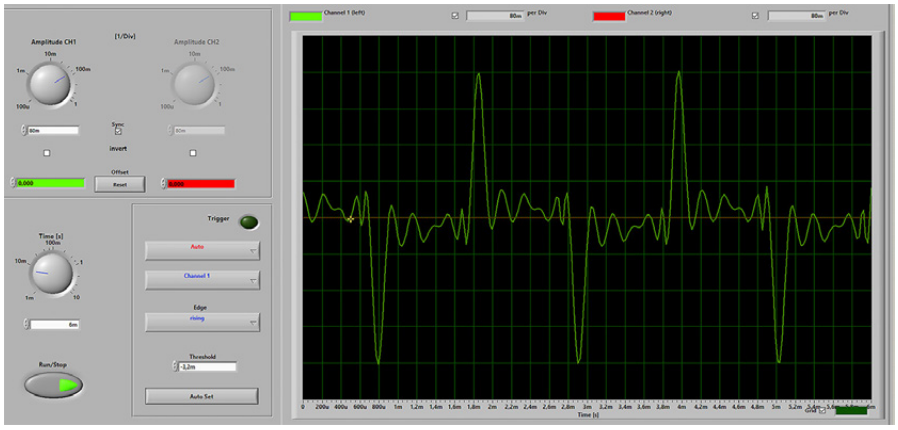

(a)

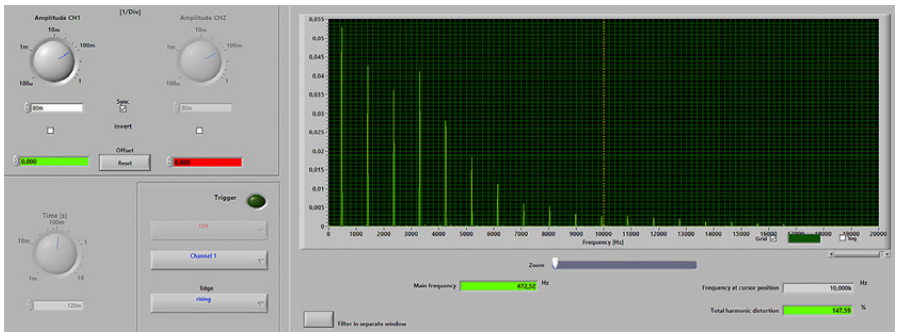

(b)

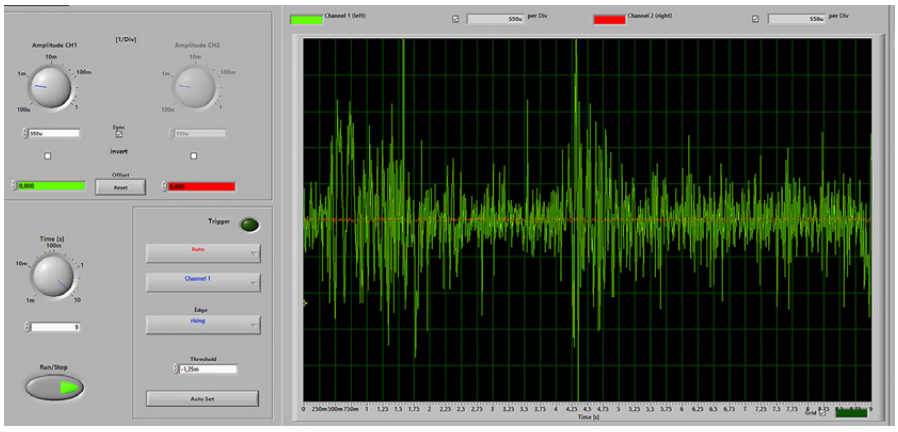

(c)

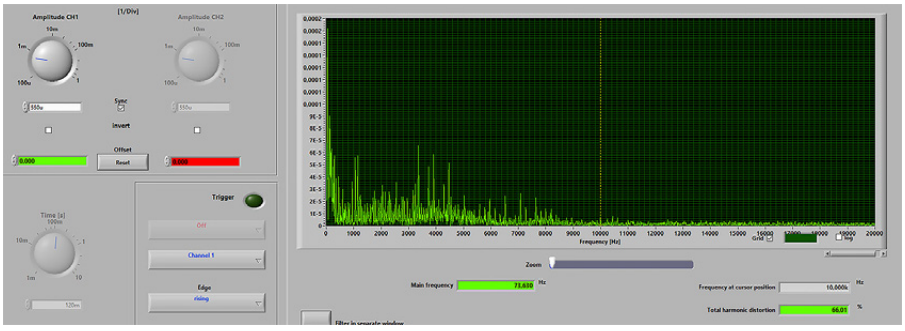

(d)

Fig. 34. Frequency-time characteristics of the research results for the positive feedback auto-compensation submodule: (a) oscillogram of the stable mode of acoustic positive feedback formation (without auto-compensation); (b) amplitude spectrum corresponding to oscillogram (a); (c) oscillogram of the stable mode of the positive feedback auto-compensation; (d) amplitude spectrum corresponding to oscillogram (c)

Fig. 35. Educational and scientific laboratory of signal radioacoustics, audiovisual systems, and technologies of RTU MIREA and VGTRK

CONCLUSIONS

The multifunctional audio signal processing module based on the ADAU1701 processor was designed and investigated in the *SigmaStudio* visual-graphical software-architectural ADSP design environment. This allowed for media systems to be tested, and the characteristics of sound processing devices to be investigated. It also enabled the debugging and correcting AFR of audio monitors, as well as the processing of audio signals and simulation of conditions of the diffuse environment of sound field propagation in a limited space. The electro-acoustic and in-channel audio measurements of the audio module were performed using specially constructed experimental benches and *RoomEQWizard* and *Soundcard Oscilloscope* automated measurement software. This was carried out using the facilities of the studio laboratory of signal radio-acoustics, audio-visual systems, and technologies at the Institute of Radio-electronics and Informatics at RTU MIREA and VGTRK[7] (Fig. 35).

The software architecture for the multifunctional audio module for media testing and debugging of audio signal systems and devices was designed on the basis of ADAU1701 ADSP processor. The experimental characteristics of submodules of the multifunctional device were obtained on the basis of bench laboratory studies which enabled the media devices to be tested in the specified spectral-dynamic and spatial-temporal ranges:

- the balance routing submodule allows the impact of noise induced on the audio channel to be reduced 20-fold, thus enabling calibration of pickup audio devices;
- the audio signal processing submodule provides compression response with dynamic range from −27 up to 18.6 dB with the possibility of equalization parameterization within the range of 0.04–18 kHz at the specified goodness and AMP/ATT levels of filters. It also provides reverberation response within the range of 0.5–3000 ms, as well as audio channel cross-division into sub-bands of 20–250 Hz, 0.25–3 kHz, and 3–20 kHz with the ability to adjust AFR within the dynamic range from −30 up to 30 dB. These elements are of particular interest for panoramic and frequency balancing of audio systems;
- the submodule of AFR/PFR auto-correction of audio monitors allows the AFR dynamic nonuniformity be reduced by 40 dB. The submodule of the electro-acoustic positive feedback auto-suppression provides notch formant suppression to −100 dB at the input dynamic range of −50 up to 80 dB without impacting AFR, since each filter of the system operates independently.

ACKNOWLEDGMENTS

The study was carried out within the framework of the research on “Radio-information systems and radio-electronic technologies” (code 170-IRI).

Authors’ contributions

A.V. Gevorsky—parametric analysis and research of a multifunctional audio module based on an ADSP processor.

M.S. Kostin—development of an architectural configuration of a multifunctional ADSP module.

K.A. Boikov—development of a test program for media testing of signal audio devices.

[7] Federal State Unitary Enterprise “All-Russia State Television and Radio Broadcasting Company” (in Russ.). https://vgtrk.ru/. Accessed February 20, 2023.

REFERENCES

1. Kostin M.S. Signal radio acoustics, audiovisual systems and technologies. In: *Science of RTU MIREA at the Present Stage: Collection of Scientific Papers of the Anniversary Scientific and Technical Conference Dedicated to the 75th Anniversary of RTU MIREA.* Moscow: RTU MIREA; 2022. P. 325–328 (in Russ.).
2. Afanas'ev A.A., Rybolovlev A.A., Ryzhkov A.P. *Tsifrovaya obrabotka signalov* (*Digital Signal Processing*). Moscow: Goryachaya liniya – Telekom; 2019. 356 p. (in Russ.).
3. Steiglitz K. *A Digital Signal Processing Primer: with Applications to Digital Audio and Computer Music.* NY, USA: Dover Publications Inc.; 2020. 320 p.
4. Pirkle W.C. *Designing Audio Effect Plugins in C++: for AAX, AU, and VST3 with DSP Theory*. 2nd ed. NY, USA: Routledge; 2019. 704 p.
5. Kovalgin Yu.A., Vologdin E.I. *Audiotekhnika* (*Audio Engineering*). Moscow: Goryachaya liniya – Telekom; 2013. 742 p. (in Russ.).
6. Petlenko D.B., Yarlykov A.D., Boikov K.A. *Analogo-tsifrovye preobrazovateli signal'nykh audiointerfeisov* (*Analog-to-Digital Converters of Signal Audio Interfaces*). Moscow: Reglet; 2023. 65 p. (in Russ.).
7. Popov O.B., Rikhter S.G. *Tsifrovaya obrabotka signalov v traktakh zvukovogo veshchaniya* (*Digital Signal Processing in Audio Broadcasting Paths*). Moscow: Goryachaya liniya – Telekom; 2012. 342 p. (in Russ.).
8. Kovalgin Yu.A., Vakhitov Sh.Ya. *Akustika* (*Acoustics*). Moscow: Goryachaya liniya – Telekom; 2022. 660 p. (in Russ.).
9. Zölzer U. *Digital Audio Signal Processing.* 2nd ed. Chippenham, England: Wiley; 2008. 340 p.
10. Self D. *Small Signal Audio Design.* 3rd ed. NY, USA: CRC Press; 2020. 784 p.
11. Cipriani A., Giri M. *Electronic Music and Sound Design: Theory and Practice with Max 8*. V. 2. 3rd ed. Rome, Italy: ConTempoNet; 2020. 748 p.
12. Kamenov A. *Digital Signal Processing for Audio Applications*. 2nd ed. Amazon. Kindle edition. RecordingBlogs; 2014. 348 p.
13. Collins K. *Studying Sound: A Theory and Practice of Sound Design Hardcover*. London, England: The MIT Press; 2020. 248 p.
14. Reiss J.D., McPherson A. *Audio Effects. Theory, Implementation and Application*. Boca Raton, USA: CRC Press; 2008. 368 p.
15. Petlenko D.B., Yarlykov A.D., Boikov K.A. *Tsifrovye metody sekvensornoi ekvalizatsii audiosignalov radioakusticheskikh system* (*Digital Methods of Sequencer Equalization of Audio Signals of Radioacoustic Systems*). Moscow: Reglet; 2023. 109 p. (in Russ.).

СПИСОК ЛИТЕРАТУРЫ

1. Костин М.С. Сигнальная радиоакустика, аудиовизуальные системы и технологии. В сб.: *Наука РТУ МИРЭА на современном этапе: сборник научных трудов Юбилейной научно-технической конференции, посвященной 75-летию РТУ МИРЭА*. М.: РТУ МИРЭА; 2022. С. 325–328.
2. Афанасьев А.А., Рыболовлев А.А., Рыжков А.П. *Цифровая обработка сигналов*. М.: Горячая линия – Телеком; 2019. 356 с.
3. Steiglitz K. *A Digital Signal Processing Primer: with Applications to Digital Audio and Computer Music.* NY, USA: Dover Publications Inc.; 2020. 320 p.
4. Pirkle W.C. *Designing Audio Effect Plugins in C++: for AAX, AU, and VST3 with DSP Theory*. 2nd ed. NY, USA: Routledge; 2019. 704 p.
5. Ковалгин Ю.А., Вологдин Э.И. *Аудиотехника.* М.: Горячая линия – Телеком; 2013. 742 с.
6. Петленко Д.Б., Ярлыков А.Д., Бойков К.А. *Аналого-цифровые преобразователи сигнальных аудиоинтерфейсов.* М.: Реглет; 2023. 65 с.
7. Попов О.Б., Рихтер С.Г. *Цифровая обработка сигналов в трактах звукового вещания*. М.: Горячая линия – Телеком; 2012. 342 с.
8. Ковалгин Ю.А., Вахитов Ш.Я. *Акустика.* М.: Горячая линия – Телеком; 2022. 660 с.
9. Zölzer U. *Digital Audio Signal Processing.* 2nd ed. Chippenham, England: Wiley; 2008. 340 p.
10. Self D. *Small Signal Audio Design.* 3rd ed. NY, USA: CRC Press; 2020. 784 p.
11. Cipriani A., Giri M. *Electronic Music and Sound Design: Theory and Practice with Max 8*. V. 2. 3rd ed. Rome, Italy: ConTempoNet; 2020. 748 p.
12. Kamenov A. *Digital Signal Processing for Audio Applications*. 2nd ed. Amazon. Kindle edition. RecordingBlogs; 2014. 348 p.
13. Collins K. *Studying Sound: A Theory and Practice of Sound Design Hardcover*. London, England: The MIT Press; 2020. 248 p.
14. Reiss J.D., McPherson A. *Audio Effects. Theory, Implementation and Application*. Boca Raton, USA: CRC Press; 2008. 368 p.
15. Петленко Д.Б., Ярлыков А.Д., Бойков К.А. *Цифровые методы секвенсорной эквализации аудиосигналов радиоакустических систем*. М.: Реглет; 2023. 109 с.

About the authors

Andrey V. Gevorsky, Student, MIREA – Russian Technological University (78, Vernadskogo pr., Moscow, 119454 Russia). E-mail: x33590@gmail.com. http://orcid.org/0009-0001-9734-7515

Mikhail S. Kostin, Dr. Sci. (Eng.), Associate Professor, Head of the Department of Radio Wave Processes and Technologies, Deputy Director, Institute of Radio Electronics and Informatics, MIREA – Russian Technological University (78, Vernadskogo pr., Moscow, 119454 Russia). E-mail: kostin_m@mirea.ru. Scopus Author ID 57208434671, RSCI SPIN-code 5819-2178, http://orcid.org/0000-0002-5232-5478

Konstantin A. Boikov, Cand. Sci. (Eng.), Associate Professor, Department of Radio Wave Processes and Technologies, Institute of Radio Electronics and Informatics, MIREA – Russian Technological University (78, Vernadskogo pr., Moscow, 119454 Russia). E-mail: bojkov_k@mirea.ru. Scopus Author ID 57208926258, RSCI SPIN-code 2014-6951, http://orcid.org/0000-0003-0213-7337

Об авторах

Геворский Андрей Владимирович, студент, ФГБОУ ВО «МИРЭА – Российский технологический университет» (119454, Россия, Москва, пр-т Вернадского, д. 78). E-mail: x33590@gmail.com. http://orcid.org/0009-0001-9734-7515

Костин Михаил Сергеевич, д.т.н., доцент, заведующий кафедрой радиоволновых процессов и технологий, заместитель директора Института радиоэлектроники и информатики ФГБОУ ВО «МИРЭА – Российский технологический университет» (119454, Россия, Москва, пр-т Вернадского, д. 78). E-mail: kostin_m@mirea.ru. Scopus Author ID 57208434671, SPIN-код РИНЦ 5819-2178, http://orcid.org/0000-0002-5232-5478

Бойков Константин Анатольевич, к.т.н., доцент, кафедра радиоволновых процессов и технологий Института радиоэлектроники и информатики ФГБОУ ВО «МИРЭА – Российский технологический университет» (119454, Россия, Москва, пр-т Вернадского, д. 78). E-mail: bojkov_k@mirea.ru. Scopus Author ID 57208926258, SPIN-код РИНЦ 2014-6951, http://orcid.org/0000-0003-0213-7337

Translated from Russian into English by Kirill V. Nazarov
Edited for English language and spelling by Dr. David Mossop